COPPE
Instituto Alberto Luiz Coimbra de Pós-Graduação e Pesquisa de Engenharia
UFRJ

POPULATION DYNAMICS AND NETWORK STRUCTURE IN THE GLOBAL CORAL-SYMBIONT NETWORK UNDER WATER TEMPERATURE VARIATIONS

Maria Gabriella Cavalcante Basílio

Dissertação de Mestrado apresentada ao Programa de Pós-graduação em Engenharia de Sistemas e Computação, COPPE, da Universidade Federal do Rio de Janeiro, como parte dos requisitos necessários à obtenção do título de Mestre em Engenharia de Sistemas e Computação.

Orientador: Daniel Ratton Figueiredo

Rio de Janeiro
Junho de 2025

POPULATION DYNAMICS AND NETWORK STRUCTURE IN THE GLOBAL CORAL-SYMBIONT NETWORK UNDER WATER TEMPERATURE VARIATIONS

Maria Gabriella Cavalcante Basílio

DISSERTAÇÃO SUBMETIDA AO CORPO DOCENTE DO INSTITUTO ALBERTO LUIZ COIMBRA DE PÓS-GRADUAÇÃO E PESQUISA DE ENGENHARIA DA UNIVERSIDADE FEDERAL DO RIO DE JANEIRO COMO PARTE DOS REQUISITOS NECESSÁRIOS PARA A OBTENÇÃO DO GRAU DE MESTRE EM CIÊNCIAS EM ENGENHARIA DE SISTEMAS E COMPUTAÇÃO.

Orientador: Daniel Ratton Figueiredo

Aprovada por: Prof. Daniel Ratton Figueiredo
Prof. Adriano Maurício de Almeida Côrtes
Prof. Flávia Maria Darcie Marquitti

RIO DE JANEIRO, RJ – BRASIL
JUNHO DE 2025

Cavalcante Basílio, Maria Gabriella

Population Dynamics and Network Structure in the Global Coral-Symbiont Network under Water Temperature Variations/Maria Gabriella Cavalcante Basílio. – Rio de Janeiro: UFRJ/COPPE, 2025.

XIV, 60 p.: il.; 29, 7cm.

Orientador: Daniel Ratton Figueiredo

Dissertação (mestrado) – UFRJ/COPPE/Programa de Engenharia de Sistemas e Computação, 2025.

Referências Bibliográficas: p. 57 – 60.

1. Population Dynamics. 2. Ecological Networks. 3. Coral Bleaching. I. Ratton Figueiredo, Daniel. II. Universidade Federal do Rio de Janeiro, COPPE, Programa de Engenharia de Sistemas e Computação. III. Título.

Ao meu pai, que vive o amor
como entrega—inteira, serena e
sem pedir nada em troca.

Agradecimentos

Agradeço aos meus pais, Jerônimo e Ero, que, com muito esforço e amor, me deram todas as oportunidades que eles mesmos não tiveram. Um agradecimento especial à minha mãe, que, desde a infância, fez questão de estudar comigo, incentivando e me ajudando a superar cada desafio. E à minha avó, por ser minha maior fã e estar sempre comigo em todos os momentos.

À minha irmã Maria Luiza, que esteve ao meu lado em todos os momentos da vida, sempre me apoiando com muito amor. Nossas conquistas sempre foram divididas e celebradas juntas, e sinto muito orgulho de tudo o que você conquistou.

Ao meu orientador, Prof. Daniel, que com muita paciência e dedicação sempre esteve disposto a ajudar e ensinar. Seu exemplo inspira a mim e a todos os seus alunos que, assim como eu, sonham em seguir a carreira acadêmica.

Agradeço também à Prof. Flávia Marquitti pela oportunidade de participar do Programa de Formação em Ecologia Quantitativa, que foi essencial para o meu desenvolvimento na ciência, e por continuar me ajudando sempre que possível.

Às minhas amigas da academia — Gabriella Dantas, Isabela Castro, Karolayne Dessabato, Tiffany Vilca e Yildiz Jordán — que se tornaram um presente na minha vida. Guardo no coração todos os momentos que compartilhamos e a inspiração que cada uma de vocês representa. Vocês sempre terão minha admiração e torcida.

Às amigas de toda a vida — Ana Carolina Herbst, Giovanna Pacheco e Júlia Pessoa — e à minha amiga mais recente, Cristiane Silva, por todas as conversas, risadas e carinho. A amizade de vocês sempre trouxe alegria e motivação para seguir em frente.

Agradeço a todos os professores que cruzaram o meu caminho, em especial ao Prof. André Loureiro, por serem fonte de inspiração e por dedicarem tanto empenho em fazer com que seus alunos alcancem seus sonhos. Sem vocês, eu não teria chegado até aqui. Agradeço também às agências brasileiras CAPES, CNPq e FAPERJ, cujo apoio por meio de bolsas e projetos de pesquisa contribuiu para a realização deste trabalho.

Por fim, ao Gabriel, pela parceria, amor e por tantas vezes ter acreditado mais em mim do que eu mesma.

Resumo da Dissertação apresentada à COPPE/UFRJ como parte dos requisitos necessários para a obtenção do grau de Mestre em Ciências (M.Sc.)

DINÂMICA POPULACIONAL E ESTRUTURA DE REDE NA REDE GLOBAL DE CORAIS E SIMBIONTES SOB VARIAÇÕES DE TEMPERATURA DA ÁGUA

Maria Gabriella Cavalcante Basílio

Junho/2025

Orientador: Daniel Ratton Figueiredo

Programa: Engenharia de Sistemas e Computação

Este trabalho investiga a dinâmica populacional e a estrutura de rede da rede global de corais e simbiontes (algas zooxantelas) sob o impacto de variações de temperatura da água. Para isso, foram desenvolvidos modelos matemáticos que descrevem o crescimento populacional de corais e simbiontes em redes bipartidas, considerando suas interações ecológicas e os efeitos do estresse térmico. Dois modelos principais foram propostos: um modelo de crescimento populacional sem capacidade de carga e outro que inclui a capacidade de carga, oferecendo uma visão mais realista das limitações ecológicas. Esses modelos incorporam explicitamente a estrutura da rede, evidenciando como a conectividade entre espécies influencia a resiliência, i.e. capacidade de um organismo – ou de uma população – de recuperar-se após sofrer uma redução em seu tamanho populacional em decorrência de perturbações térmicas, dos corais e de seus simbiontes diante de eventos repetidos de aumento de temperatura. Por meio de análises numéricas em diferentes regiões oceânicas, o trabalho avalia as dinâmicas populacionais em redes reais e em redes aleatórias. Os resultados indicam que a estrutura da rede tem impacto significativo nas dinâmicas populacionais: corais geralmente mostram maior resiliência ao estresse térmico do que os simbiontes, e a complexidade e a conectividade da rede influenciam a capacidade das populações de resistirem a eventos de aquecimento. Além disso, as redes reais se mostraram mais sensíveis a perturbações do que as redes aleatórias, ressaltando a importância de conservar as interações ecológicas naturais. Este estudo gera insights a respeito dos efeitos das mudanças climáticas sobre a rede simbiótica coral-alga e avalia a resiliência ecológica dos recifes de corais em um cenário de mudanças globais.

Abstract of Dissertation presented to COPPE/UFRJ as a partial fulfillment of the requirements for the degree of Master of Science (M.Sc.)

POPULATION DYNAMICS AND NETWORK STRUCTURE IN THE GLOBAL CORAL-SYMBIONT NETWORK UNDER WATER TEMPERATURE VARIATIONS

Maria Gabriella Cavalcante Basílio

June/2025

Advisor: Daniel Ratton Figueiredo

Department: Systems Engineering and Computer Science

This work investigates the population dynamics and network structure of the global coral and symbiont network (zooxanthellae algae) under the impact of water temperature variations. For this purpose, mathematical models were developed that describe the population growth of corals and symbionts in bipartite networks, considering their ecological interactions and the effects of thermal stress. Two main models were proposed: a population growth model without carrying capacity and another that includes carrying capacity, offering a more realistic view of ecological limitations. These models explicitly incorporate network structure, evidencing how connectivity between species influences the resilience, i.e. the ability of an organism – or a population – to recover after suffering a reduction in its population size due to thermal disturbances, of corals and their symbionts to repeated temperature rise events. Using numerical analyses in different oceanic regions, the work evaluates population dynamics in real networks and in random networks. The results indicate that network structure has a significant impact on population dynamics: corals generally show greater resilience to thermal stress than symbionts, and network complexity and connectivity influence the ability of populations to withstand warming events. In addition, real networks were shown to be more sensitive to disturbances than random networks, highlighting the importance of conserving natural ecological interactions. This study generates insights into the effects of climate change on the coral-algae symbiotic network and assesses the ecological resilience of coral reefs in a scenario of global change.

Contents

List of Figures

List of Tables

Chapter 1

Introduction

The oceans are home to an astonishing diversity of life forms. In this vast marine world, ecosystems are shaped by complex interactions between species, ranging from predator-prey dynamics to various forms of mutualism. These relationships are essential not only for the survival of individual organisms, but also for maintaining ecological balance. Among the many associations in marine environments, one of the richest biologically and ecologically is the symbiotic relationship between reef-building corals and microscopic photosynthetic algae known as zooxanthellae.

Coral reefs are vibrant ecosystems that thrive primarily in shallow tropical and subtropical waters. Despite occupying a small portion of the ocean floor, they are home to a wide variety of marine species, providing habitat, breeding grounds, and protection. This extraordinary biodiversity is largely sustained by the mutualistic bond between corals and their algal partners. Zooxanthellae reside in the coral tissues, where they photosynthesize and produce organic compounds that serve as a crucial energy source for the host coral. In return, the algae receive shelter and access to nutrients contained in the corals' metabolic waste.

This relationship is not only essential to the health of individual corals, but also the basis for reef building. The energy provided by algae enables corals to build enormous reef structures over time. These structures, in turn, provide habitat for a huge variety of marine life, protect coastlines from erosion, and support fishing and tourism industries around the world. The ecological and economic value of coral reefs is therefore closely linked to the success of the symbiosis between corals and algae.

However, this relationship is extremely sensitive to changes in environmental conditions. The balance between corals and algae depends on a narrow window of physical and chemical parameters, especially temperature. When sea surface temperatures rise even slightly above typical maximums for long periods, the physiological stress experienced by the coral-algae association can lead to the breakdown of the symbiosis (DONNER *et al.* [2], WILLIAMS e PATTERSON [3]). Under ther-

mal stress, zooxanthellae produce substances that are harmful to both partners. As a defense mechanism, the coral expels the algae from its tissues, leading to a drastic loss of pigmentation. This phenomenon, known as coral bleaching, is not merely the disappearance of beautiful landscapes—it is a sign of metabolic perturbation and a prelude to potential mortality.

The implications of coral bleaching extend far beyond the loss of color. Once expelled, microalgae may not return or may be replaced by species that form less efficient symbiotic associations. Without their primary source of energy, bleached corals suffer from reduced growth and reproduction rates and are more susceptible to disease. The prolonged bleaching can result in partial or complete mortality of coral colonies. Reefs that experience widespread bleaching lose structural complexity, which reduces their ability to support marine life. As reef ecosystems collapse, the species that depend on them—from small invertebrates to large predatory fish—are forced to migrate, adapt, or perish. The ecological chain reactions triggered by coral bleaching can therefore lead to drastic changes in community composition and loss of biodiversity.

Furthermore, the consequences of reef degradation are not limited to the oceans. Coral reefs benefit millions of people around the world. They act as natural barriers that reduce the impact of waves, helping to protect coastlines from storms and erosion. Their biological wealth supports artisanal and commercial fisheries, which serve as a vital source of food and economic resources for coastal communities. Coral reefs also support marine tourism industries, contributing significantly to the economies of many tropical countries. When reefs bleach and die, all of this is reduced or lost, increasing the vulnerability of human populations that depend on healthy marine ecosystems.

The increasing frequency and intensity of bleaching events in recent decades are strongly linked to climate change. Global warming, driven by rising concentrations of greenhouse gases in the atmosphere, is raising ocean temperatures at an unprecedented rate. This warming is compounded by local stressors such as pollution, overfishing and coastal development, which further undermine reef resilience. Bleaching events are recurrent and have become more frequent in the last decade (HUGHES *et al.* [4]), affecting reefs in nearly every ocean basin.

Despite the challenges posed by rising ocean temperatures, there is considerable variability in how organisms respond to environmental stress. Differences in physiological, genetic, and ecological characteristics can influence tolerance levels, with some species exhibiting greater resistance than others. For instance, certain traits may enhance an organism's capacity to withstand stress, such as structural adaptations or more effective defense mechanisms. Similarly, within a single species or functional group, different subtypes may display varying degrees of resilience and

efficiency under changing conditions (WILLIAMS e PATTERSON [3], SWAIN *et al.* [5]). This diversity is essential for understanding potential adaptive responses and the resilience of ecosystems in the face of climate change.

Moreover, several studies have highlighted the capacity for organisms to adjust their symbiotic associations over time. These shifts may occur in response to environmental fluctuations, seasonal cycles, or stress events such as bleaching (ROWAN *et al.* [6], GLYNN *et al.* [7], TOLLER *et al.* [8]). This notion—that symbiotic partnerships can reorganize following disturbances—has been formalized as the adaptive bleaching hypothesis BUDDEMEIER e FAUTIN [9]. Rather than interpreting bleaching solely as a pathological breakdown of the symbiosis, this hypothesis proposes that it may serve as a regulatory and adaptive mechanism: stress-induced dissociation from a symbiont opens a window for the host to establish new partnerships, potentially with algal types that are better suited to prevailing environmental conditions. According to this study, such reassortment of host-symbiont combinations enables rapid physiological adjustment without requiring genetic evolution in either partner. Over time, this dynamic flexibility may explain both the persistence of coral through repeated environmental oscillations and the apparent ecological stability of coral reef systems despite their sensitivity to short-term stressors. In this view, bleaching—though disruptive in the short term—may ultimately promote long-term resilience by facilitating symbiotic adaptation BUDDEMEIER e FAUTIN [9].

However, the extent of this flexibility is limited. While some hosts can harbor multiple symbiont types simultaneously, not all combinations are functionally compatible or equally beneficial WEIS *et al.* [10]. Even when shifts in symbiont composition occur, they may come with trade-offs. For instance, certain symbionts can enhance thermal tolerance and support host survival during stressful periods, but this often comes at the cost of reduced growth, lower energy transfer, or diminished reproductive output under more stable conditions JONES e BERKELMANS [11], LITTLE *et al.* [12]. These limitations indicate that symbiotic flexibility, while potentially advantageous in the short term, may not always translate into long-term benefits, and its adaptive value depends heavily on the surrounding environmental context.

This ability to reorganize their symbiotic communities makes corals fascinating organisms, showing that they have biological mechanisms to try to adapt. Still, these changes don't always come without a cost. By switching symbiotic partners, a coral can alter its growth rate, its ability to reproduce, and even the physical structure of its colony. This means that even when a coral survives the heat, it can become less efficient at building the reef around it—and this affects the entire marine ecosystem that depends on these structures.

Therefore, coral survival depends not only on water temperature, but also on a complex network of biological interactions, the diversity of algae available in the environment, and the physiological flexibility of each coral species. Understanding these dynamics is essential to predict which populations are most likely to resist changes and to guide conservation strategies that take into account biological resilience, not just the physical environment.

In this context, the present study proposes a mathematical model that captures coral-algae growth dynamics, incorporating their symbiotic relationship and thermal responses under recurring warming events. This research aims to provide insights into the interactions between corals and algae when exposed to environmental stress (in particular, water temperature variations) and contribute to a better understanding of how reef systems can be preserved in a rapidly changing world.

1.1 Main Contributions

This study presents some important contributions to the understanding of coral–symbiont network dynamics under repeated thermal stress. First, two mathematical models were proposed with the aim of capturing the population dynamics within these symbiotic networks, considering the network structure. The first model considers population growth without an upper limit, while the second incorporates a carrying capacity, providing a more ecologically realistic representation of natural population limitations.

By explicitly integrating network structure into the population growth equations, the models offer a framework for analyzing how connectivity patterns shape the resilience of coral–algal systems in the face of environmental stressors. Here, resilience is understood as a property of population dynamics—specifically, the capacity of a population to recover after experiencing declines caused by thermal disturbances. It refers to the ability of the population to resume growth or restore its size over time following episodes of thermal disturbances. Connectivity, in this context, refers to the number of links a given node has within the network—that is, the number of neighbors with which it interacts, also known as the node's degree. This integration highlights the crucial role of mutualistic interactions in determining species survival and system stability. The numerical solution of these equations reveals that network structure—specifically node degrees and the connectivity of neighboring nodes—has significant effects on population outcomes.

The study also assesses the impact of disrupting biological affinities through network randomization. Comparisons between real and randomized networks demonstrate that shuffling the natural symbiotic connections reduces system stability, emphasizing the ecological importance of preserving authentic interaction patterns.

Additionally, extensive numerical results of the proposed models were conducted across multiple regional networks, providing an evaluation of how species-specific traits and network-level factors modulate resilience under repeated warming events.

1.2 Organization

This dissertation is organized into six chapters. Chapter 1 introduces the study's objectives, motivation, and context, and presents the main contributions and the organization of the dissertation. Chapter 2 reviews the fundamental concepts and related work, including population dynamics, network models, types of symbiotic relationships, coral bleaching, and previous studies relevant to the coral–symbiont network. Chapter 3 details the construction of the global coral–symbiont network, focusing on its structure and degree distributions. Chapter 4 presents the first population growth model, its mathematical formulation, and results regarding population dynamics and the influence of network structure. Chapter 5 presents another model that incorporate carrying capacity, providing a more realistic ecological scenario, and discusses the corresponding numerical results and insights. Finally, Chapter 6 concludes the dissertation by summarizing the key findings, discussing their implications, and proposing future research directions.

Chapter 2

Concepts and Related Work

2.1 Populational growth

The study of population dynamics is crucial to ecological theory. In the literature, there are a wide variety of models proposed to describe how populations grow, interact and respond to environmental conditions. Classical approaches generally rely on differential equations to represent population changes over time, while more recent models incorporate other factors such as spatial heterogeneity, environmental variability and evolutionary processes.

One of the earliest and most widely used models is the logistic growth model, originally proposed by VERHULST [13] and later popularized by PEARL e REED [14]. This model describes population growth as a function of the current population size and a carrying capacity, with the slowing of growth interpreted as a consequence of intraspecific competition—that is, individuals of the same species competing for limited resources. Its popularity is largely due to its simplicity and clear biological interpretation. However, empirical studies—such as those conducted by SMITH [15] on *Daphnia magna*—demonstrated that real populations often deviate from logistic behavior due to temporal discrepancies and other factors. To address this issue, SMITH [15] developed an alternative model based on empirical data from controlled experiments using expanding cultures, introducing a new formulation that explicitly considers metabolic substitution rates and the effects of size structure.

In natural ecosystems, populations rarely exist in isolation. Instead, they are embedded in networks of interactions that include competition, predation, parasitism, and mutualism. These interactions are fundamental to population regulation and community dynamics and have been extensively explored through mathematical modeling.

One of the classic approaches to modeling interspecific interactions is the Lotka-Volterra framework (LOTKA [16, 17]), originally developed in the 1920s to de-

scribe predator-prey dynamics. In its simplest form, this model assumes that the prey population grows exponentially in the absence of predators, while the predator population declines in the absence of prey. The interaction term couples the two populations through a linear functional response, representing the predation rate. Although elegant, this model has limitations. These limitations have led to the development of more detailed models, such as the Rosenzweig-MacArthur model (ROSENZWEIG e MACARTHUR [18]), which incorporates prey carrying capacity and functional saturation responses.

Another important class of models is the competition model that often extend the logistic growth model to include terms representing the negative effect of one species on another. For example, in the two-species Lotka-Volterra competition model (widely presented in KOT [19] and MURRAY [20]) the growth rate of each species is reduced not only by its own density but also by the density of its competitor, scaled by a competition coefficient. These models predict outcomes such as competitive exclusion, stable coexistence, or priority effects, depending on the intrinsic growth rates of the species and the intensity of the interaction.

Mutualistic interactions, such as those between pollinators and plants or between host corals and their symbiotic algae, can be modeled by incorporating terms that increase the growth rate of each species as a function of the density of the partner species. These models often include saturated interaction benefits or costs, to avoid runaway positive feedbacks. For example, HOLLAND e DEANGELIS [21] proposed models of mutualism with tradeoffs that balance benefit and cost over a range of densities, capturing more realistic dynamics.

These models illustrate the evolution of ecological thinking from simple, homogeneous systems to more realistic, structured models that integrate space, evolution, and environmental change. They serve as essential tools for understanding persistence, extinction, and adaptation—key concerns in ecology and conservation biology.

2.2 Network models

Network models have emerged as powerful tools for exploring complex biological systems, offering a structured way to represent and analyze the interactions between individual units such as species, populations, or habitats. In the context of ecology and evolutionary biology, these models provide a framework to understand not only the structure of biological systems but also their dynamic behavior in response to environmental and internal perturbations.

A notable example of this approach is the work by BASTOLLA *et al.* [22], who developed an analytical framework to explore how the structure of mutualistic networks influences biodiversity. Focusing on plant–pollinator systems, the authors

showed that the nested architecture commonly found in empirical networks plays a key role in reducing effective interspecific competition. By incorporating network topology into a dynamical model of population interactions, they demonstrated that more nested networks promote higher species coexistence compared to random or compartmentalized structures. Their results also revealed that nestedness emerges naturally when new species preferentially associate with generalist partners, minimizing their competitive load. This study highlights how structural properties of ecological networks, such as nestedness, are not merely descriptive features but can actively shape the stability and diversity of ecological communities.

Ecological networks also play a critical role in conservation biology. VERBOOM *et al.* [23] applied network models to assess how climate-induced increases in environmental variability affect species persistence. Their numerical evaluations demonstrated that networks with large, well-connected habitat patches are more resilient to extinction under variable conditions. The network structure was essential to evaluate how spatial configuration influences population viability and to develop robust design criteria for ecological reserves.

Network models are also used to study migratory species, whose life cycles span multiple geographically disjoint habitats. Taylor and Norris (2010) developed a graph-based model to simulate the population dynamics of migratory animals across breeding and wintering sites. Their results demonstrated how the structure and connectivity of migratory networks—along with the associated costs of migration—influence both local population sizes and global species persistence. The network perspective was crucial to uncovering these context-dependent outcomes.

Overall, these studies demonstrate how network models allow for a more integrated and dynamic understanding of biological systems. They allow the exploration of how spatial, temporal, and evolutionary processes interact across multiple scales.

2.3 Symbiotic Relationship

The term symbiosis was first introduced by BARY [24] to describe the close associations between fungi and algae in lichens, defining it as "the living together of two dissimilar organisms". Over time, the definition has expanded to include a wide range of interactions that may include beneficial, harmful, and neutral outcomes, and that can change over time and in different environmental contexts.

Essentially, symbiosis refers to a prolonged and close biological association between two or more distinct species (BARY [24]). This association can occur intracellularly or extracellularly and may involve direct physical contact or functional interdependence (by biochemical or ecological means). It is important to emphasize that the nature of the symbiotic relationship often cannot be understood by study-

ing organisms in isolation, but through the interaction of these organisms with a complex system (RELMAN [25]).

2.3.1 Types of Symbiotic Relationship

Symbiotic associations are generally classified into three main categories, based on the ecological or evolutionary outcomes for the partners involved: mutualism, commensalism, and parasitism. These categories do not necessarily represent fixed states, but rather can change over time depending on environmental conditions.

Mutualism

In mutualistic relationships, both organisms benefit from the interaction, which can lead to strong interdependence. In some cases, this reciprocal advantage becomes so essential that the association turns obligate, meaning neither species can thrive—or even survive—without the other. A classic example in marine systems is the mutualistic interactions between chemosynthetic bacteria and deep-sea invertebrates that enable life in otherwise inhospitable environments (DUBILIER *et al.* [26]).

Commensalism

Commensalism describes relationships in which one organism benefits while the other remains unaffected. These associations are often transient or facultative and may be difficult to detect or quantify. Furthermore, the distinction between commensalism and mutualism or parasitism can be ambiguous, since apparently neutral interactions can cause subtle long-term effects or change under conditions of stress or disease. An example is the microbial communities in the human gut that derive nutrients or habitat without significantly impacting the host's health or physiology under normal conditions but contribute to disease in dysbiotic states (DETHLEFSEN *et al.* [27], LEY *et al.* [28]).

Parasitism

In parasitic associations, one organism benefits at the expense of another. Parasites typically exploit the host's resources, often causing damage. Some parasites develop complex mechanisms to evade host immunity or manipulate their reproduction, as observed in the *Wolbachia* bacteria, which infects arthropods and nematodes (WERREN *et al.* [29]).

Therefore, symbiosis represents a fundamental organizing principle in biology,

highlighting the interconnectedness of life and the importance of cooperation, competition, and coadaptation.

2.4 Coral Bleaching

Coral reef ecosystems are among the most diverse and productive environments on Earth, largely due to the mutualistic symbiosis between reef-building corals (*Scleractinia*) and microalgae of the genus *Symbiodinium*, commonly referred to as zooxanthellae. These unicellular algae reside in the tissues of their host coral, forming a critical relationship for the nutrition, calcification, and overall resilience of the coral in nutrient-poor tropical waters (MUSCATINE e PORTER [30]). Through photosynthesis, zooxanthellae translocate a large portion of the fixed carbon to the coral, while in return receiving inorganic nutrients, protection, and access to light in the shallow marine environment (FALKOWSKI *et al.* [31]).

However, this symbiosis is extremely sensitive to environmental disturbances. Coral bleaching refers to the physiological response to stress in which corals expel their symbiotic algae that are usually responsible for their coloration, resulting in the characteristic bleaching of coral tissue (GLYNN [32]). Bleaching seriously compromises the health of corals, reducing growth and reproduction, and increasing susceptibility to disease and mortality if the stress conditions persist (HOEGH-GULDBERG [33]).

Figure 2.1: Comparison between a bleached coral (left) and a health coral (right). Photo from XL Catlin Seaview Survey team [1]

Among the various stressors linked to coral bleaching, increased sea surface temperature stands out as the most significant and well-documented cause. Numerous mass bleaching events have been strongly correlated with anomalous thermal stress, particularly those associated with El Niño–Southern Oscillation (ENSO) events (HOEGH-GULDBERG [33], HUGHES *et al.* [34]).

The breakdown of symbiosis through bleaching has profound ecological consequences, as it can lead to widespread coral mortality, reef degradation, and biodi-

versity loss. Bleached reefs provide reduced habitat and food supplies for associated organisms, leading to cascading effects throughout the reef ecosystem (GRAHAM *et al.* [35]). On an evolutionary scale, recurrent bleaching events exert selective pressures on both host corals and symbionts. There is growing interest in the potential for thermal tolerance through symbiont switching or shuffling, whereby corals associate with more thermally resilient *Symbiodinium* clades (BAKER [36]). However, such adaptive responses may be limited and insufficient to keep pace with climate change.

2.5 Related work

This section brings together the topics discussed above by integrating real-world data, temperature fluctuations, and mathematical modeling. Recent studies have increasingly used network analysis to understand how rising ocean temperatures affect the structure and development of coral reef systems. A notable work studies the global network between coral species and *Symbiodiniaceae* and its resistance to temperature stress as well as its robustness to temperature perturbations (WILLIAMS e PATTERSON [3]). Another recent work proposes and evaluates an eco-evolutionary model that shows that shortcuts in the dispersal network (e.g., corals that disperse larvae throughout the ocean to coral reefs) across environmental gradients (i.e., changes in non-living factors through space or time) hinder the persistence of population growth across regions (MCMANUS *et al.* [37, 38]). These works have been quite successful in identifying how the network structure affects the sensitivity of corals to changes in water temperature, either in symbiotic associations networks or in dispersal networks.

For instance, in the context of the global coral-symbiont network (WILLIAMS e PATTERSON [3]), null networks were created by altering physiological parameters of organisms or the network structures. A bleaching model was developed with weighted links representing temperature thresholds for host–symbiont pairs. Resistance to temperature stress and ecological robustness were assessed by analyzing how different networks responded to increasing temperatures (e.g., link removal) and species (e.g., node) removal. Results indicated that robustness to bleaching and other perturbations varied across spatial scales and differed from null networks. The global coral–symbiont network was more sensitive to environmental attacks, such as rising temperatures, with symbionts providing more stability than hosts. Network structure and thermal tolerances are not represented by uniform random patterns, making the system more vulnerable to environmental changes.

The dispersal networks represent demographic connectivity between populations located in different habitats. These networks describe how offspring of species move

between these habitats, forming connections that influence both the demography and the growth of populations (MCMANUS *et al.* [37, 38]). Additionally, through the eco-evolutionary model, it was observed that random networks performed better in non-evolving populations, while regular networks favored populations with higher evolutionary potential (MCMANUS *et al.* [37]). These networks, by reducing maladaptive gene flow, allowed local populations to adapt more efficiently. Results reinforce the importance of considering eco-evolutionary dynamics, network structures, and environmental gradients when assessing species' ability to migrate and persist under climate change.

Chapter 3

Global Coral-Symbiont Network

Data from the GeoSymbio database (FRANKLIN *et al.* [39]) and a complementary database compiled by WILLIAMS e PATTERSON [3] were used to construct the bipartite coral–symbiont network. The GeoSymbio database provides extensive information on symbiotic associations, including the *Symbiodinium* type (based on ITS2 sequence), the scientific names (genus and species) of both coral hosts and symbionts, and the oceanic region where each association sample was collected. In total, 53 distinct ocean regions are represented in the GeoSymbio dataset, offering a broad geographic distribution of host–symbiont interactions.

To complement these structural data with functional information, the database assembled by WILLIAMS e PATTERSON [3] was used to incorporate thermal tolerance values for both corals and symbionts. Thermal tolerance in this context refers to the relative ability of each organism to withstand elevated water temperatures without experiencing physiological collapse or bleaching. These values were derived from the ranking proposed by SWAIN *et al.* [5], which aggregates experimental evidence from multiple studies to produce a unified and comparative scale. The resulting index is dimensionless and normalized between 0 and 1, where 0 indicates extreme sensitivity to thermal stress and 1 denotes high resistance to bleaching. Unfortunately, the database is not complete and some organisms do not have a specified thermal tolerance. In such cases, the mean value of the thermal tolerance was used as a reference.

To construct the final bipartite network, the information from both datasets was combined into a single file. This integrated table includes, for each coral–symbiont pair, their taxonomic identification, geographic region of occurrence, and assigned thermal tolerance values. The resulting dataset not only defines the structure of the network but also provides key biological attributes to each network node. For reproducibility, the merged dataset is available in a public GitHub repository linked to this dissertation and can be accessed here.

Based on this combined dataset, a bipartite network encoding the relationship

between host corals and their endosymbiotic algae was generated. In this representation, a link corresponds to the symbiotic association between a symbiont species and a host species (Fig. 3.1). Each node in the network represents a species in a specific region, such that if a given coral or symbiont species occurs in k distinct regions, it is represented by k separate nodes in this network.

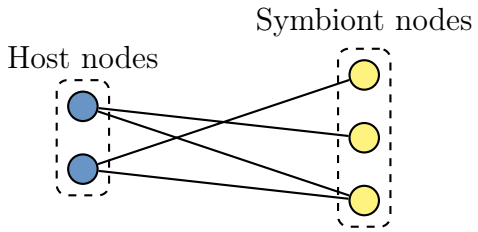

Figure 3.1: Bipartite coral–symbiont network with host nodes (blue) and symbiont nodes (yellow).

3.1 Network Structure and Characteristics

The global coral–symbiont network has 867 symbiont nodes and 1178 host nodes, 2747 links and 181 connected components. Note that the connected components are at least the number of ocean regions (i.e., 53), however the global network has many more connected components. Hence, there are multiple connected components within the same ocean region.

Moreover, five connected components of the global network each corresponding to a different region were chosen to be analyzed separately, as shown in Table 3.1. These regions represent the most threatened regions of coral bleaching in the oceans. Note that these networks have a different number of nodes and links, but relatively similar density, where density is the ratio of the number of edges to the maximum possible number of edges in the graph.

Table 3.1: Network nodes and links in different connected components analyzed.

Region	**Symbiont nodes**	**Host nodes**	**links**	**Density**
Great Barrier Reef	76	198	415	0.055
Phuket	36	152	442	0.162
Western Indian	43	131	337	0.120
Western Caribbean	36	61	111	0.101
Florida	26	32	75	0.180

3.2 Degree Distribution

The degree of the global coral-symbiont network is analyzed, considering all 53 ocean regions. Table 3.2 shows that the average degree of both types of nodes is relatively similar but not the standard deviation, which is larger for the symbiont nodes. Furthermore, since the minimum degree is 1, there are no isolated organisms (nodes) in the coral-symbiont network.

Table 3.2: Degree in the global coral–symbiont network.

Type of node	Standard Deviation	Minimum degree	Average degree	Maximum degree
Symbiont	8.306	1	3.168	102
Host	2.346	1	2.332	51

Fig. 3.2 shows the complementary cumulative distribution function for the degree of both symbiont and host nodes. Note that both distributions are heavy-tailed since a tiny number of symbionts are connected to 100 or more hosts and a tiny number of hosts are connected to 50 or more symbionts. Further, note that the symbionts have a heavier tail (the distribution curve decreases more slowly) indicating that symbionts connect more, also because the number of host nodes is much larger.

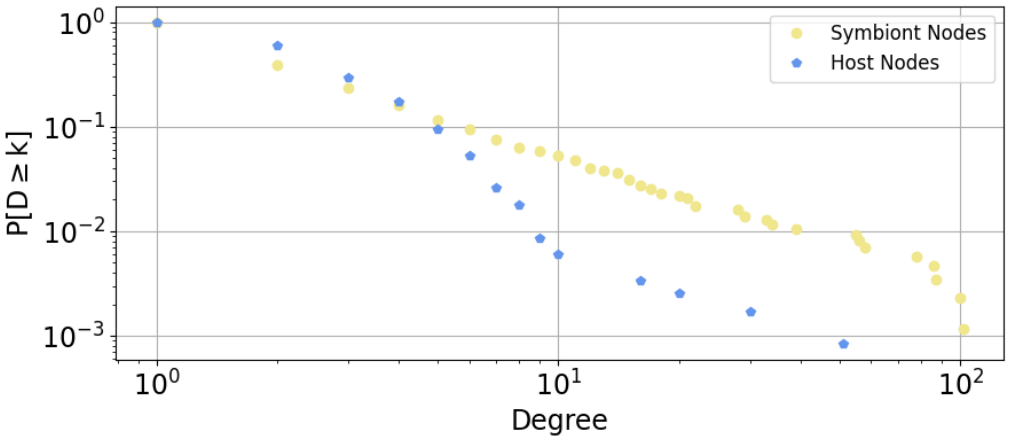

Figure 3.2: The complementary cumulative distribution function of symbiont and host nodes.

Moreover, the difference between the tail values and the average degree values of the two types of nodes is very significant. Recall that the average degree of the symbionts and hosts are approximately 3 and 2, respectively. Thus, the majority of hosts and symbionts are specialists (have very few connections) while a tiny amount of both nodes are generalists (have large number of connections).

Chapter 4

Population Growth Model in Networks

This chapter presents the first mathematical model proposed in this thesis in order to represent the population growth of different species while capturing network structure and water temperature variations.

4.1 Mathematical model

In essence, the model is a system of coupled ordinary differential equations to track the population size of symbionts and hosts over time. This model considers the coral-symbiont network, where every node has associated with it a population size. Note that this model uses a single variable per node instead of a variable for each symbiotic relationship (i.e., links). Consequently, this model has significantly fewer variables (see Table 3.1). However, network links drive the population dynamics as growth of corals and algae are coupled and symbiotic.

Let $S_i(t)$ and $H_j(t)$ denote the population size of symbiont i and host j at time t, respectively. These are the only variables in the model, all other quantities are parameters. The population dynamics (derivative) of S_i over time is given by:

$$\frac{dS_i}{dt} = r_i^s S_i + \frac{S_i}{|N_i^s|}\left(\frac{r_i^s}{1+e^{-\gamma_c(c_i^s(t)-\bar{c_0^s})}}\right) - S_i m_i^s \tag{4.1}$$

Note that there is a growth term (positive) and a mortality term (negative) that are driven by a growth rate (r_i^s) and mortality rate (m_i^s). Moreover, the growth term also depends on the network structure. This is the main contribution of the proposed model. In particular, the growth rate also depends on the population size of the corals that have a symbiotic relationship (link) with this symbiont, i.e., the interaction between neighboring nodes.

Table 4.1: Definition for symbols of variables and parameters of the model.

Symbol	Definition (variables and parameters)
$S_i(t)$	population size of the i-th symbiont species at time t
$H_j(t)$	population size of the j-th host species at time t
n_s	number of symbiont species in the network
n_h	number of host species in the network
N_i^s	neighborhood of the i-th symbiont species
N_j^h	neighborhood of the j-th host species
$\|N_i^s\|$	degree of the i-th symbiont species
$\|N_j^h\|$	degree of the j-th host species
r_i^s	growth rate of the i-th symbiont species
r_j^h	growth rate of the j-th host species
m_i^s	mortality rate of the i-th symbiont species
m_j^h	mortality rate of the j-th host species
τ_i^s	thermal tolerance of the i-th symbiont species
τ_j^h	thermal tolerance of the j-th host species

The influence of the network on symbiont i is given by:

$$c_i^s(t) = \sum_{j \in N_i^s} \frac{\ln(H_j(t)+1)}{|N_j^h|} \tag{4.2}$$

Where each host j connected to symbiont i (i.e., $j \in N_i^s$) contributes a term given by the logarithm of its population size, $\ln(H_j(t)+1)$ (with a logarithmic transformation to compress the scale), divided by $|N_j^h|$. Dividing the population size of an organism by its degree assumes that each population interacts uniformly with the population of neighboring organisms. This normalization ensures that the interaction of a symbiont or host population is distributed evenly among its connections. Moreover, this assumption significantly simplifies the model as it requires a single variable (population size) for each node while also capturing network heterogeneity (different degrees).

The growth rate (r_i^s) is then added to a logistic factor $\left(\frac{r_i^s}{1+e^{-\gamma_c(c_i^s(t)-c_0^s)}}\right)$ that depends on $c_i^s(t)$ (Eq. 4.2) and reaches its maximum at r_i^s. This logistic formulation acts as a regulatory mechanism that limits the contribution of the interaction term, ensuring that it does not drive the organism's growth beyond its biologically plausible maximum. In practice, the interaction term is summed with the intrinsic growth rate of the species, but its effect is constrained so that population growth remains within physiologically realistic bounds. Biologically, the term $\frac{S_i}{|N_i^s|}\left(\frac{r_i^s}{1+e^{-\gamma_c(c_i^s(t)-c_0^s)}}\right)$ can be interpreted as the effective strength of the pairwise interaction between sym-

biont i and host j. Note that the first term $\left(\frac{S_i}{|N_i^s|}\right)$ does not depend on j, as this represents the fraction of population S_i interacting with host H_j.

The midpoint of the logistic curve ($\bar{c_0^s}$) is defined as the average initial influence over all symbionts, given by:

$$\bar{c_0^s} = \frac{1}{n_s} \sum_{i=1}^{n_s} c_i^s(0) \tag{4.3}$$

where n_s is the total number of symbiont nodes and $c_i^s(0)$ is a model parameter. This value represents the average of the initial c_i^s values across all symbionts at the beginning of the numerical analysis (i.e., at $t = 0$). At this initial time point, all symbionts are assigned a population size of $c_i^s(0) = 1000$, and all hosts begin with a population size of $c_j^h(0) = 100$.

The growth rate (r_i^s) is given by:

$$r_i^s = \frac{r_0^s}{\sqrt{2\pi}} . e^{\left(\frac{-\gamma_r (T(t)-z)^2}{\left(\tau_i^s\right)^2}\right)} \tag{4.4}$$

While the mortality rate (m_i^s) is given by:

$$m_i^s = \begin{cases} \mu, & \text{if } T(t) \leq z \\ \\ 1 - e^{\left(\frac{-\gamma_m (T(t)-z)^2}{\left(\tau_i^s\right)^2}\right)} + \mu, & \text{if } T(t) > z \end{cases} \tag{4.5}$$

Note that both the growth and mortality rates have already been proposed in the literature (MCMANUS *et al.* [37], WALSWORTH *et al.* [40]) and depend on the current local sea temperature ($T(t)$) and thermal tolerance (τ_i^s) of each organism.

However, some adjustments were made to the growth and mortality rates. Initially, the growth rate included the term $\frac{r_0^s}{\sqrt{2\pi(\tau_i^s)^2}}$, introducing an unintended duality into the model. On one hand, a higher thermal tolerance (τ_i^s) means that the exponential term $e^{\left(-\gamma_r \frac{(T(t)-z)^2}{(\tau_i^s)^2}\right)}$ decays more slowly, contributing positively to the growth rate. However, at the same time, this higher thermal tolerance also increases the denominator of the term $\frac{r_0^s}{\sqrt{2\pi(\tau_i^s)^2}}$, thereby reducing the overall growth rate. As a result, the growth rate could paradoxically be lower for symbionts with higher thermal tolerances.

To resolve this issue and avoid the conflicting effects of thermal tolerance, the denominator was simplified by removing the thermal tolerance term, resulting in $\frac{r_0^s}{\sqrt{2\pi}}$. This change ensures that the beneficial effect of thermal tolerance—slower

decay of the exponential term—remains the sole driver of its influence on the growth rate.

Finally, damping coefficients (γ_r in Eq. 4.4 and γ_m in Eq. 4.5) were introduced. These coefficients control the rate at which the exponential terms decay, allowing the model to better capture the resilience of populations to environmental fluctuations.

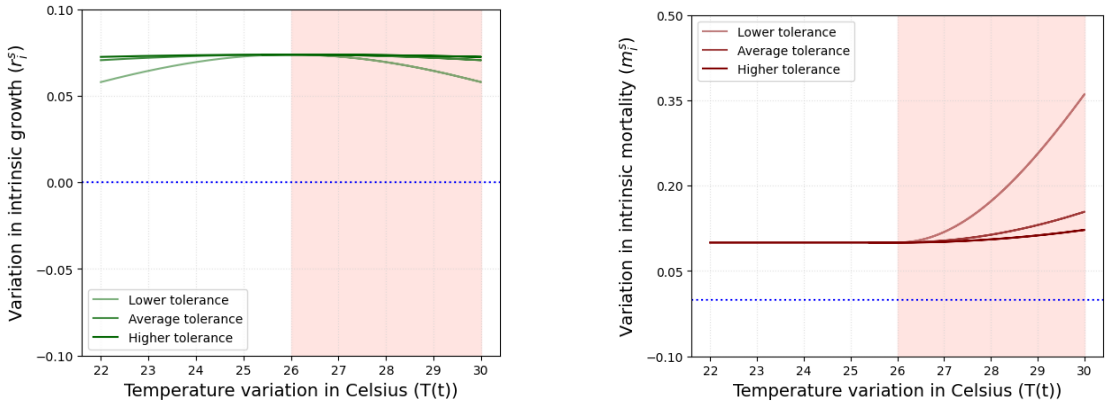

(a) Growth rate of symbionts

(b) Mortality rate of symbionts

Figure 4.1: Variation in growth (left) and mortality (right) rates of symbionts with different thermal tolerance values (τ_i^s) across different temperatures. The red zone in the plot mark when the system is above the optimal temperature for growth ($T(t) > z$) and the blue dotted line represents r_i^s and m_i^s equals to zero.

Figure 4.1(a) illustrates how the growth rate of symbionts responds to changes in temperature. As expected, the maximum growth rate occurs at 26°C, which is defined as the optimal temperature for growth (z). The curve is symmetrical around this point, indicating that deviations above or below the optimum lead to a similar reduction in growth. The figure also highlights differences among organisms with varying thermal tolerances. Symbionts with higher thermal tolerance maintain relatively high growth rates across the full temperature range, whereas those with lower tolerance show consistently reduced growth, regardless of the temperature.

Figure 4.1(b) shows how the mortality rate changes across different temperature values. The plot reveals distinct behaviors depending on whether the temperature is below or above the optimal growth temperature. When the temperature is equal to or below z, the mortality rate remains constant at μ (as defined in Table 4.2). In contrast, when the local sea temperature exceeds the optimum, mortality increases according to a function that depends on the organism's thermal tolerance.

Finally, the population dynamics (derivative) of H_j over time is given by:

$$\frac{dH_j}{dt} = r_j^h H_j + \frac{H_j}{|N_j^h|}\left(\frac{r_j^h}{1 + e^{-\gamma_c(c_j^h(t) - \bar{c_0^h})}}\right) - H_j m_j^h \tag{4.6}$$

Note that this equation is identical to Eq. 4.1 making the model symmetric. The growth rate, the term dependent on the network structure and mortality rate for hosts are also given by equations Eq. 4.4, Eq.4.2, Eq.4.3 and Eq. 4.5, respectively (replacing superscript s with h and subscript i with j, as shown in Table 4.2). Thus, there is no inherent population growth advantage between symbionts and hosts. Of course, their growth depends on the parameters of the model such as network structure, thermal tolerance, water temperature and initial population size.

Table 4.2: Parameter definitions and values used in the numerical evaluation.

Parameter	**Value**	**Definition**
r_0^s	0.185	scaling factor for symbionts' growth rate
r_0^h	0.185	scaling factor for hosts' growth rate
z	26°C	optimum growth temperature for symbionts and hosts
μ	0.1	the base mortality rate
γ_r	$8 \cdot 10^{-4}$	damping coefficient for growth
γ_m	10^{-3}	damping coefficient for mortality
γ_c	10^{-2}	damping coefficient for interaction

The parameters r_0^s and r_0^h were used in the MCMANUS *et al.* [37] article with values equal to 1. Furthermore, the base mortality was used in MCMANUS *et al.* [37] with a value equal to zero and used in WALSWORTH *et al.* [40] with a value equal to 0.1.

The growth and mortality rate of symbionts and hosts depend on the current local sea temperature. Thus, a model for the variation of the sea temperature is needed. The temperature model used in this work was based on real ocean temperature data, collected over 26 months, in two regions of Western Australia: Coral Bay and Tantabiddi (FULTON *et al.* [41]) which is shown to be recurrent. In particular, the temperature model is given by:

$$T(t) = 4\cos\left(\frac{t}{75} + 22\right) + 26 \tag{4.7}$$

The choice of parameters for the temperature model was arbitrary to emulate recurrence within a temperature range and timescale. Fig. 4.2 shows the variation of the temperature over time, indicating the sucessive warming events.

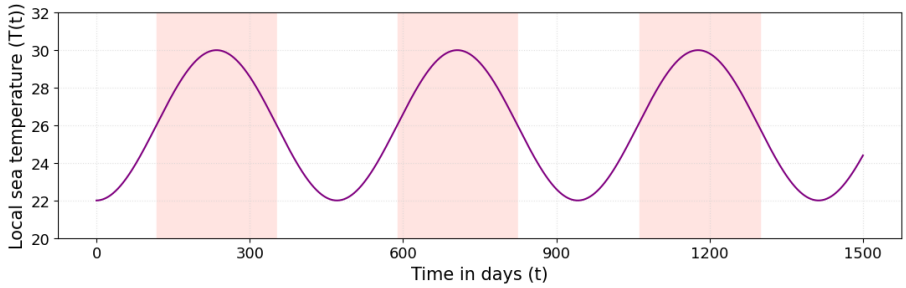

Figure 4.2: Local sea temperature function over time. The red colored zones mark when the environment is heating up $(T(t)) > z$).

Finally, Eq. 4.1 and Eq. 4.6 will be solved numerically and independently for each region (see Table 3.1) according to the above temperature model over a time horizon that simulates successive warming events over 1500 days, as shown in Fig. 4.2.

4.2 Results

The numerical solution of the population model offers valuable insights into how the populations of host corals and their endosymbiotic algae respond when exposed to successive warming events, especially when their growth is intricately linked through the network of interactions. By solving these coupled dynamics, it is possible to explore not only how individual species behave but also how the structure of the network shapes the overall population trajectories over time. This approach allows us to investigate how the network structure influences the resilience and recovery of these populations after thermal stress events.

To explore how network structure shapes population trajectories, every population began with non-zero initial sizes: each symbiont was set to 1,000 individuals and each host species to 100. This uniform initialization removes any initial advantage among species, so differences that emerge over time can be attributed to network structure and model parameters rather than to unequal starting conditions. The coupled systems of differential equations for symbionts and hosts (Eqs. 4.1–4.6) were solved numerically, region by region, with Python's `scipy.integrate.odeint`. Identical parameter values were applied to all regions, so any variation in population growth or collapse reflects network structure and initial conditions alone. The full implementation, including data loading, parameter settings, and `odeint` calls, is available here.

4.2.1 Population Dynamics

As illustrated in Figure 4.3, symbionts generally exhibit a declining trend in their population dynamics over time. Although there is some oscillatory behavior driven by temperature fluctuations, the overall trend is for all populations to decline, approaching zero over time. This declining trend reflects the combined effects of environmental stress and the inherent vulnerability of symbiotic relationships under heat stress.

However, as illustrated in Table 4.3, there is a small subset of symbiont types that manage to overcome this general decline and instead exhibit a growing trend over time. These symbionts are able to escape the downward trajectory observed in most species, persisting and even increasing in size for a longer period before facing potential collapse, or in some cases, avoiding extinction altogether. This observation is particularly interesting because it highlights the influence of network structure in shaping symbiont population dynamics in different regions. It suggests that certain network structures may help to mitigate the effects of temperature perturbations by allowing some symbiont species to thrive despite challenging overall conditions.

Furthermore, as shown in Figure 4.4, the population dynamics of host coral species reveal a trend that contrasts significantly with that of their endosymbiotic algae. Across all regions analyzed, host species are more likely to exhibit more sustained population growth over time compared to symbionts (see Table 4.3). This trend suggests that, under the same thermal disturbance scenarios, hosts tend to be more resilient and able to maintain viable population sizes compared to their symbiotic partners. Such a result points to important differences in the way these two groups of organisms respond to environmental stress, highlighting the complexity of their interactions within the network.

This resilience observed in host species can be attributed to a combination of biological and network-related factors. One of the most relevant biological factors is the thermal tolerance of the hosts themselves. According to the parameter values used in our model, host species exhibit a wide range of thermal tolerance values (τ_i^h), ranging from 0.136 to 0.997, with a mean of 0.706. These values are, in general, higher than those of their symbiotic algae (τ_i^s), which range from 0.210 to 0.843, with a mean of 0.519. This difference implies that host corals, on average, have a greater inherent capacity to cope with higher temperatures and repeated thermal disturbances than their endosymbiotic partners. This characteristic is favored in the proposed model, since a higher thermal tolerance implies a higher growth rate (see Eq. 4.4 and Fig. 4.1(a)) and a lower mortality rate (see Eq. 4.5 and Fig. 4.1(b)). As a consequence, they are less likely to suffer immediate population collapses under heat stress.

In addition to these biological differences, the structure of the interaction network itself also plays a crucial role in shaping host population dynamics. As illustrated in Fig. 3.2 and 3.2, host nodes tend to have fewer connections (i.e., fewer neighboring nodes) than symbiont nodes. This lower connectivity can have significant implications for the propagation of disturbances through the network. Specifically, as will be discussed in Table 4.5, species with lower connectivity may suffer less from the negative effects that may arise from the decline of neighboring species. For host corals, this means that they are less exposed to the indirect effects of symbiont population collapse.

This difference in network connectivity highlights the importance of considering not only the specific characteristics of each species, but also the broader ecological context in which these species interact. The way in which hosts are embedded in the symbiotic network determines their vulnerability or resilience to environmental changes. In scenarios where symbionts suffer a sharp decline, the relative isolation of hosts within the network may be favorable, allowing them to maintain their population sizes.

Taken together, these findings highlight the complex interplay between biological traits and network structure in determining species resilience. The observed ability of host corals to sustain and even increase their population sizes in the face of repeated warming events suggests that they may play a key role in maintaining the overall stability of coral-algal symbiosis under climate change scenarios. Such resilience is likely a crucial factor in the long-term persistence of coral reef ecosystems.

Table 4.3: Percentage of species that became extinct over the course of population dynamics in the different regions.

Region	**Symbiont species**	**Host species**
Great Barrier Reef	96.1%	66.2%
Phuket	97.2%	86.8%
Western Indian	97.7%	89.3%
Western Caribbean	100%	45.9%
Florida	92.3%	56.2%

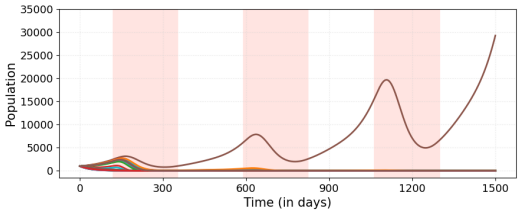

(a) Symbionts at Great Barrier Reef in linear scale

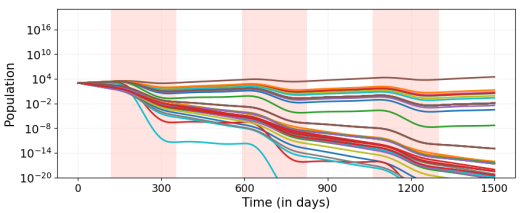

(b) Symbionts at Great Barrier Reef in semi-log scale

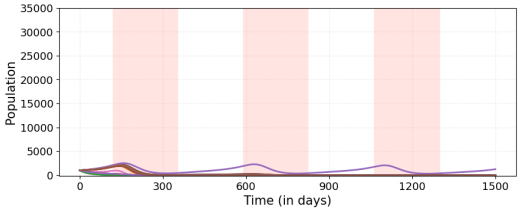

(c) Symbionts at Phuket in linear scale

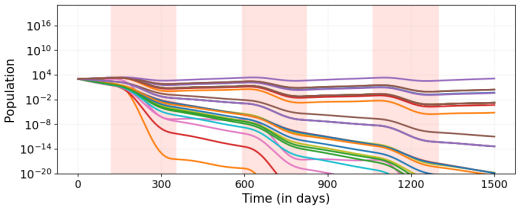

(d) Symbionts at Phuket in semi-log scale

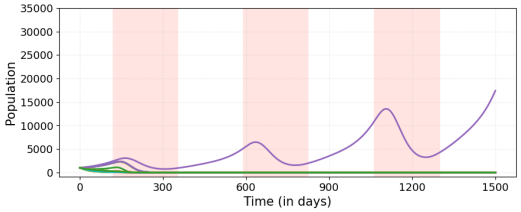

(e) Symbionts at Western Indian in linear scale

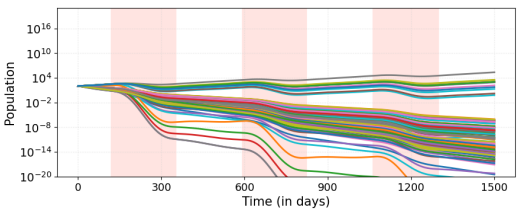

(f) Symbionts at Western Indian in semi-log scale

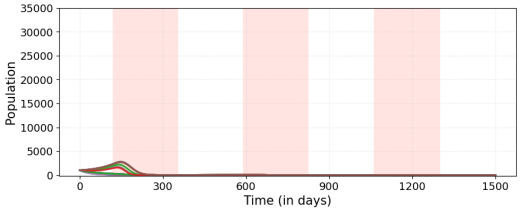

(g) Symbionts at Western Caribbean in linear scale

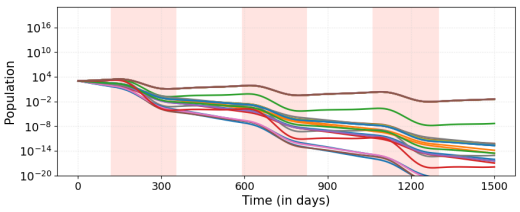

(h) Symbionts at Western Caribbean in semi-log scale

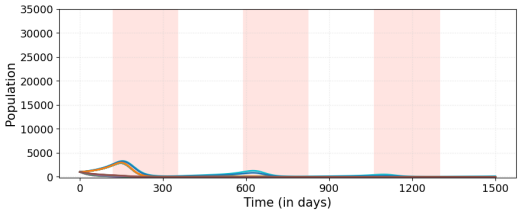

(i) Symbionts at Florida in linear scale

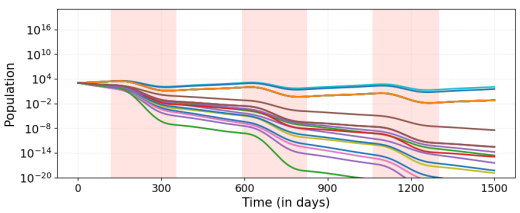

(j) Symbionts at Florida in semi-log scale

Figure 4.3: Population dynamics of symbiont species in the five regions studied (Table 3.1). On the left, linear scale plots with identical y-axis ranges facilitate comparisons across regions. On the right, semi-log plots (logarithmic y-axis) reveal different population size magnitudes over time. Red colored zones mark when the environment is heating up ($T(t)) > z$).

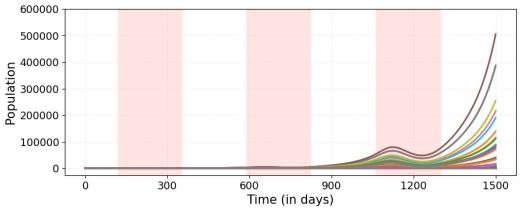

(a) Hosts at Great Barrier Reef in linear scale

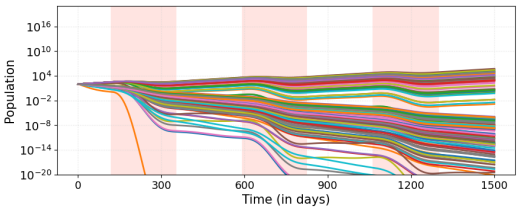

(b) Hosts at Great Barrier Reef in semi-log scale

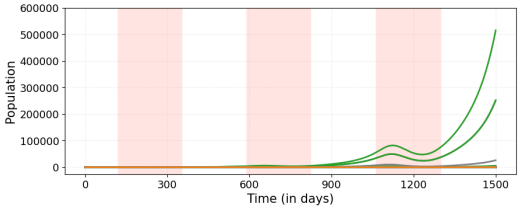

(c) Hosts at Phuket in linear scale

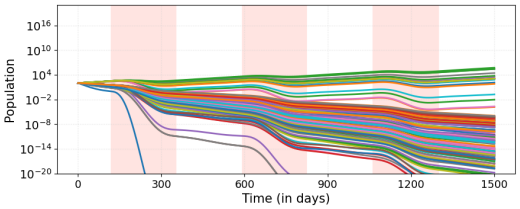

(d) Hosts at Phuket in semi-log scale

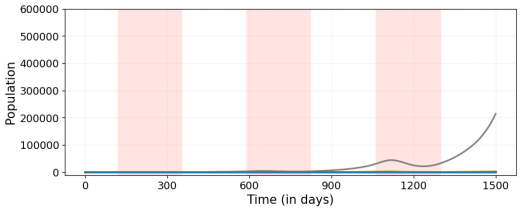

(e) Hosts at Western Indian in linear scale

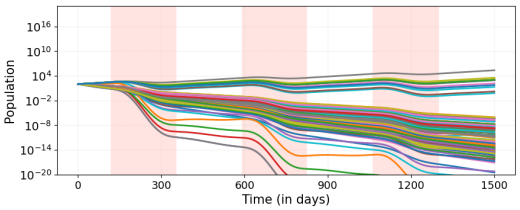

(f) Hosts at Western Indian in semi-log scale

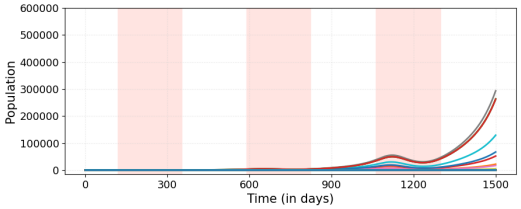

(g) Hosts at Western Caribbean in linear scale

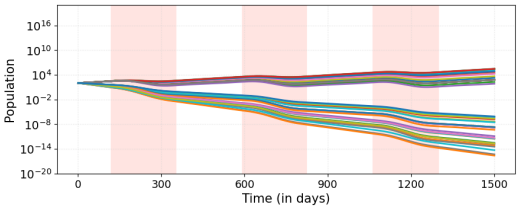

(h) Hosts at Western Caribbean in semi-log scale

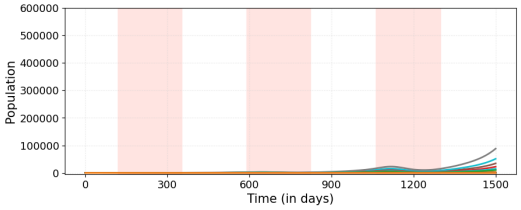

(i) Hosts at Florida in linear scale

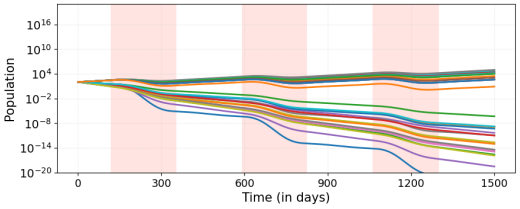

(j) Hosts at Florida in semi-log scale

Figure 4.4: Population dynamics of host species in the five regions studied (Table 3.1). On the left, linear scale plots with identical y-axis ranges facilitate comparisons across regions. On the right, semi-log plots (logarithmic y-axis) reveal different population size magnitudes over time. Red colored zones mark when the environment is heating up $(T(t)) > z$).

Nevertheless, even when all species begin with the same initial population sizes, differences in their population trajectories emerge due to the interplay between the network structure and the thermal tolerances of each species. Since the network is not uniform—some nodes have higher degrees than others—population growth is not uniform either. This variation in network connectivity is reflected in the complementary cumulative distribution function of node degrees for each region (Fig. 4.5). Specifically, the complementary cumulative distribution function for symbionts (Fig. 4.5(a)) shows that larger networks exhibit heavy-tailed degree distributions, indicating the presence of highly connected nodes that can significantly influence network dynamics. In contrast, smaller networks of symbionts do not display such heavy-tailed patterns. For host nodes, none of the networks display heavy-tailed degree distributions (Fig. 4.5(a)). Moreover, since all networks have more host nodes than symbiont nodes (see Table 3.1), symbionts are generally more connected than hosts. This difference in connectivity can lead to distinct responses to environmental disturbances and influence the overall resilience of the network.

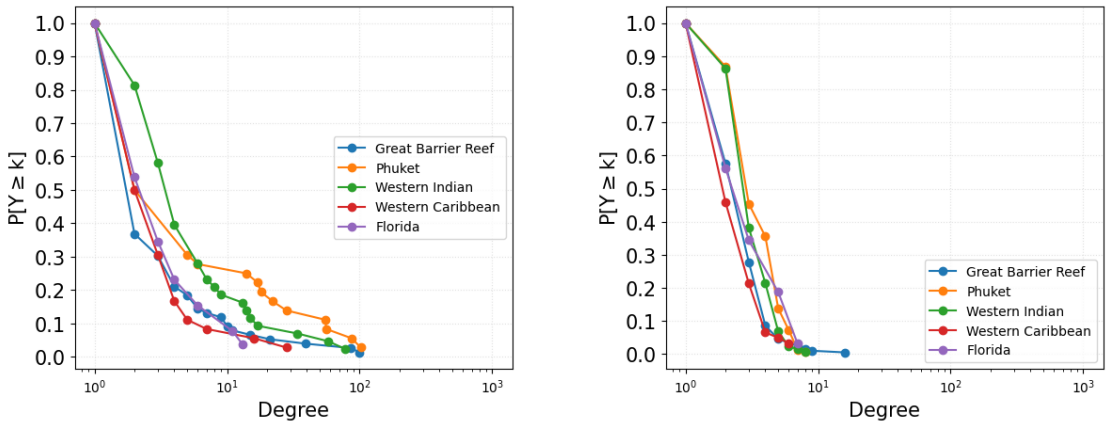

(a) Degree distribution of symbionts in different regions

(b) Degree distribution of hosts in different regions

Figure 4.5: Complementary cumulative distribution function of symbiont nodes (left) and host nodes (right) degree in different regions

Figure 4.6 shows the population size distributions after 830 days—immediately following the second warming event—for both symbionts and host corals across all regions analyzed. The choice of $t = 830$ was deliberate to ensure that the differences in the orders of magnitude of each population size were more balanced, making it easier to compare the different species and regions. Notably, the population size distribution of hosts exhibits a heavy tail in every region, indicating that while most species maintain small population sizes, a few species achieve disproportionately large population sizes. This highlights the key role of network structure in shaping

population dynamics, as it determines how species interactions influence resilience.

Interestingly, the symbiont population sizes also exhibit a heavy-tailed distribution, reflecting the same underlying network influence as the hosts. This result underscores that, even with identical initial conditions, the network's structure drives differences in population size outcomes for both groups. These findings emphasize the need to consider both species-specific traits and the ecological interaction network to fully understand the dynamics and resilience of coral-algal symbioses in a changing climate.

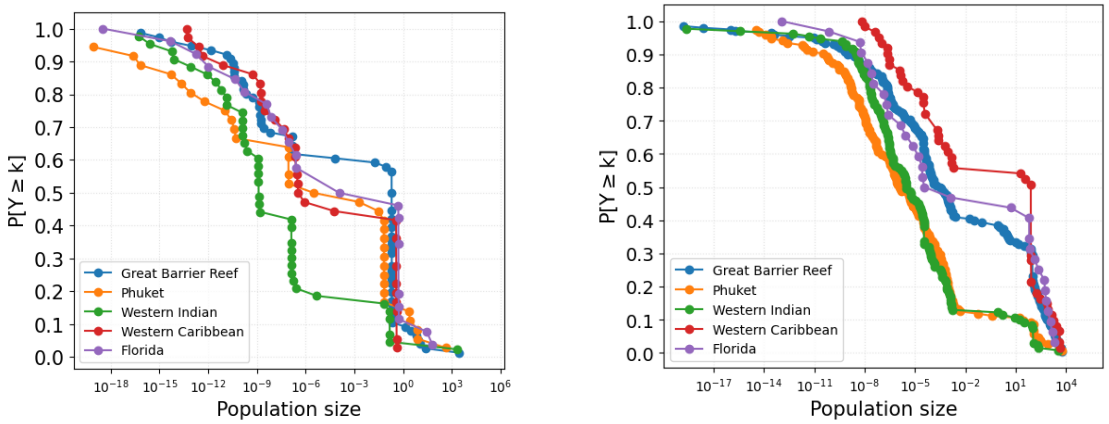

(a) Distribution of symbiont population sizes in the real network

(b) Distribution of host population sizes in the real network

Figure 4.6: Complementary cumulative distribution function of symbionts' (left) and hosts' (right) population sizes (at time $t = 830$) in their respective collection region in the real networks.

To further investigate how network structure itself modulates the resistance of species to thermal stress, we conducted additional numerical analysis using randomized networks. Here, resistance is understood not as a biological trait of individual organisms, but as a property of population dynamics—specifically, the ability of a population to maintain positive growth or avoid collapse even under repeated thermal disturbances. Specifically, to test whether the arrangement of interactions within the network influences species' resistance to thermal disturbances, we generated a random bipartite network for each region following the methodology proposed by WILLIAMS e PATTERSON [3]. In this procedure, each original link was randomly repositioned among the nodes, effectively breaking any biological symbiotic affinity while keeping both the number of links and the total number of nodes constant for each network. Moreover, the randomization ensured that no nodes were left disconnected (minimum degree of one), and all numerical analysis for these randomized networks were run using the same parameter values as those for the

real networks (see Table 4.2), ensuring a fair comparison between real and randomized network scenarios. The full implementation, including data loading, parameter settings is available here.

Figure 4.7 presents the complementary cumulative distribution function of population sizes—evaluated at time $t = 830$—in one instance of the randomized networks. The choice of $t = 830$ was made because, at this point, population sizes tend to be more balanced across orders of magnitude, allowing for a clearer interpretation of the complementary cumulative distribution function plots and a more meaningful comparison of species performance.

When comparing these randomized networks with the real ones (Fig. 4.6), it is clear that the complementary cumulative distribution function of symbiont population sizes in the randomized networks generally displays a lighter tail. For example, none of the regions' networks in the randomized case reached population sizes between 10^3 and 10^6. In contrast, the complementary cumulative distribution function of the real networks shows that symbionts in all regions, except Western Caribbean, achieve population sizes within this range. Moreover, the complementary cumulative distribution function plots for host population sizes in the randomized networks remain quite similar to those from the real networks, with all regions exhibiting consistent patterns of distribution.

This similarity in the complementary cumulative distribution functions of host population sizes across real and randomized networks may be due to inherent characteristics of the network structure itself. Notably, every regional network has a significantly higher number of host nodes compared to symbiont nodes. As a result, during the link randomization process, host nodes have fewer options for link repositioning than symbionts, which restricts the variability in their node degrees. Consequently, the overall connectivity patterns of host nodes in the randomized networks may remain similar to those in the real networks, explaining the observed consistency in the complementary cumulative distribution functions of hosts between these scenarios.

This contrast between randomized and real networks highlights the critical role of network structure in shaping population dynamics and resilience. The loss of structured symbiotic relationships in the randomized networks underscores how essential it is to preserve biological interaction patterns when assessing coral-algal populations' responses to repeated warming events. Additionally, it is worth mentioning that the complementary cumulative distribution function plots for both real and randomized networks do not necessarily start at $P[Y \geq k] = 1$ because species with near-zero population sizes were removed to focus on biologically meaningful population sizes. To ensure consistent visual interpretation, we also limited the x-axis to 10^{-20} across all plots.

Altogether, these findings emphasize that both the structure of species interactions and individual traits—such as thermal tolerance—play a fundamental role in determining the resilience of coral-algal symbioses to recurrent thermal stress.

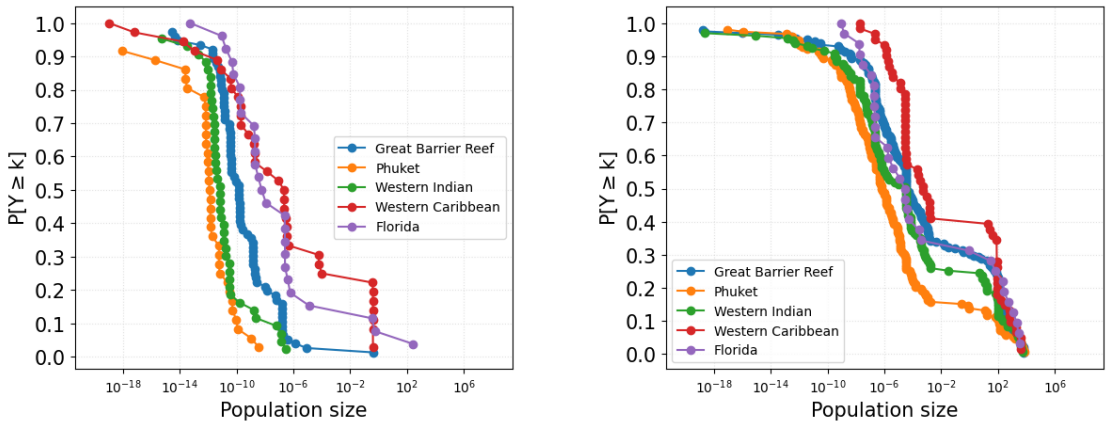

(a) Distribution of symbiont population sizes in the random network

(b) Distribution of host population sizes in the random network

Figure 4.7: Complementary cumulative distribution function of symbionts' (left) and hosts' (right) population sizes (at time $t = 830$) in their respective collection region in the random networks.

4.2.2 Influence of Network Structure

The role of network structure and species' thermal tolerances in shaping population size outcomes can also be studied through correlation analysis. By assessing the relationship between these factors and the size of populations achieved by each species, we can better understand how both intrinsic traits and network connectivity influence species resilience. In all cases, these relationships are quantified using Pearson correlation coefficients.

Table 4.4 presents the correlation coefficients between thermal tolerance and population size (at time $t = 830$) across all regions. Notably, these correlations are consistently high, indicating that species with greater thermal tolerance tend to achieve larger population sizes after the numerical evaluation. To ensure a fair analysis, the correlation was calculated between the logarithm of the population sizes (at time $t = 830$), rather than the raw population sizes. This transformation compresses the scale of the data and makes the population dynamics more linear, given that populations that grow exponentially become linear on a logarithmic scale. Moreover, this step helps balance the differences in magnitude between the population sizes and the thermal tolerance values (which range between 0 and 1). Without this transformation, the magnitude of the population size data could have dominated

the correlation calculation, potentially overshadowing the role of thermal tolerance in driving population growth.

Table 4.4: Correlation between population sizes (at time $t = 830$) and thermal tolerances in the different regions.

Region	**Symbiont nodes**	**Host nodes**
Great Barrier Reef	0.392	0.550
Phuket	0.767	0.596
Western Indian	0.612	0.579
Western Caribbean	0.256	0.076
Florida	0.485	0.454

In contrast, Table 4.5 presents the correlation between the population size at time $t = 830$ of species and their node degrees across different regions. Notably, for most regions, the correlation values are below -0.3 (which is generally considered a moderate negative correlation) for both symbionts and hosts. Biologically, this suggests that specialist species—those with fewer connections—tend to achieve higher population sizes compared to generalist species with many connections. In the context of thermal stress, this implies that species with fewer partners (specialists) are better able to sustain or even grow their populations than generalists, who might be more vulnerable to fluctuations in the environment.

This counterintuitive result can be explained by the structure of the mathematical model used to simulate these interactions. In particular, Eq. 4.2 defines the interaction term that represents the symbiotic relationship between microalgae (symbionts) and host corals. This term is expressed as the sum of the fractions of the populations of host species connected to a given symbiont species S_i, divided by the number of neighboring hosts. While symbionts with more neighbors receive a larger number of portions being added in this sum, this sum is then divided by the symbiont's degree (see Eq. 4.1), which effectively diminishes the benefit of having many connections. As a result, symbionts with fewer connections avoid this weakening effect and receive a greater contribution from each host, facilitating their population growth.

The same logic applies to hosts as well: since both equations are symmetric (see Eqs. 4.6 and 4.1), specialists with fewer neighbors tend to experience stronger individual contributions, promoting their population growth. Therefore, the negative correlation between degree and population size at time $t = 830$ observed in most regions is consistent with the mathematical formulation of the model and highlights the nuanced role of network structure in shaping species' resilience to environmental stress.

Additionally, correlations between node degrees and population sizes at time $t = 830$ were calculated using 50 instances of random networks generated for each of the analyzed regions. In these random networks, links were redistributed randomly while preserving the original number of nodes and links in each region. This procedure removed any structural patterns that could potentially influence population dynamics, enabling an assessment of whether the real network structure genuinely affects population size distributions or whether the observed patterns could simply result from network density and the number of nodes and links.

The results indicate that, in the random networks, the structure does not exhibit sufficiently strong patterns to maintain the significant negative correlations observed for the symbionts in the real networks of the Great Barrier Reef, Phuket, and Western Indian regions. In other words, the random redistribution of links dilutes any structural effects that might influence symbiont population dynamics in these regions.

Conversely, for the hosts in these same regions, strong negative correlations persist even in the random networks. This can be explained by the higher number of hosts compared to symbionts, which limits the repositioning possibilities for links in the host nodes. Consequently, the structure of the host connections remains less affected by the randomization process.

It is also important to note that the random networks exhibit considerable variation among the 50 samples, as reflected in the standard deviations reported in the Table 4.5. These standard deviations highlight the stochasticity inherent in the randomization process and underscore that the randomized networks do not reproduce the same consistent correlation patterns observed in the real networks. This further emphasizes the role of network structure in shaping population dynamics and suggests that real-world network structures play a crucial role in maintaining the observed correlations between node degree and population size.

Table 4.5: Correlation between population sizes (at time $t = 830$) and node degrees in the different regions. For the random network, the sample average correlation and its standard deviation is reported using 50 independent instances of the random network.

Region	**Real network**		**Random network**	
	Symbionts	Hosts	Symbionts	Hosts
Great Barrier Reef	-0.410	-0.481	-0.149 ± 0.055	-0.367 ± 0.047
Phuket	-0.390	-0.445	-0.094 ± 0.126	-0.252 ± 0.082
Western Indian	-0.428	-0.520	-0.192 ± 0.128	-0.421 ± 0.065
Western Caribbean	-0.572	-0.871	-0.396 ± 0.055	-0.012 ± 0.160
Florida	-0.682	-0.788	-0.560 ± 0.098	-0.016 ± 0.192

Finally, Table 4.6 presents the correlation between the sum of the degrees of each species' neighbors and their population sizes at time $t = 830$. Similar to the correlation observed with node degree, this analysis also reveals significant negative values for both symbionts and host nodes across most regions. This finding underscores that having neighbors with many connections can actually hinder population growth for both types of species in this system.

This result can be understood by examining the mathematical formulation of the model. The growth of the symbionts, determined by the network structure through Eq.4.2, is directly influenced by the degrees of the neighboring host nodes. In particular, the interaction term includes the sum of fractions of the host populations, each fraction being inversely proportional to the degree of the respective host species (the denominator term $|N_j^h|$ in Eq. 4.2). When a symbiont's neighboring hosts have a high degree, each fraction becomes smaller due to this larger denominator, effectively reducing the contribution from each neighbor. Consequently, symbionts connected to hosts with lower degrees receive larger fraction sums, which in turn enhance their growth rates.

The same logic applies to the hosts themselves, since their growth rates are influenced by the degrees of their neighboring symbionts in a similar manner. Thus, the negative correlation between the sum of neighbor degrees and population size reinforces the idea that specialists—those species embedded in simpler, less connected local neighborhoods—tend to thrive better in this model than those in highly connected, complex environments.

This pattern highlights how not only a species' own degree but also the connectivity of its neighbors can significantly impact population dynamics. It emphasizes that in mutualistic networks, resilience is not solely determined by the number of direct connections a species has but also by how connected its partners are, underlining the intricate role of network structure in ecological dynamics. Furthermore, the correlations presented in Tables 4.5 and 4.6 were also computed using the logarithm of the population sizes at time $t = 830$, following the same logic presented in the calculations of Table 4.4.

Table 4.6: Correlation between population sizes (at time $t = 830$) and sum of degrees of neighbors in the different regions.

Region	**Symbiont nodes**	**Host nodes**
Great Barrier Reef	-0.417	-0.411
Phuket	-0.397	-0.437
Western Indian	-0.459	-0.320
Western Caribbean	-0.656	-0.165
Florida	-0.717	-0.471

In addition to the correlation analyses, plots to visually illustrate how the population dynamics of both symbionts and hosts unfold across the networks were made. These plots help to understand how network structure influences species' resilience in a more intuitive way.

The networks analyzed share several symbiont and host species in common, but to focus the analysis and maintain consistency, four symbiont types (D1, C1, C3 and D1a) that are present in all networks and three host species (*Pocillopora damicornis*, *Acropora tenuis* and *Acropora valida*) that are present in all region networks, except Western Caribbean, were selected to be analyzed. These selected symbionts and host species were exposed to the same thermal variation conditions across all networks, ensuring that any differences observed are not due to differences in environmental stress. Moreover, each symbiont's and host's thermal tolerance remained constant regardless of the region in which the organism was found. Thus, the only factor that varied among the networks was the structure of interactions, which was measured using metrics such as node degree and sum of neighbors' degree.

As detailed in the table below, each of these symbionts (Tab. 4.7) and hosts (Tab. 4.8) exhibits different degrees and sum of neighbors' degrees depending on the network. These structural differences affect how each species interacts with others and, ultimately, how its population grows or declines over time.

Hence, Figs. 4.8 and 4.9 demonstrate how the population dynamics of both symbionts and hosts change when the degree and the sum of the degrees of their neighbors differ from one network to another. This approach assesses how variations in network structure—independent of species traits like thermal tolerance—shape population trajectories and potentially influence community resilience under repeated thermal stress events.

Table 4.7: Structural characteristics (node degree and sum of neighbor degrees) of the same types of symbionts that were found in different regions (Fig. 4.8). Thermal tolerance values for these types are D1: 0.662, C1: 0.466, C3: 0.510 and D1a: 0.419.

	Node degree				**Sum of neighbors' degree**			
Symbiont type	**D1**	**C1**	**C3**	**D1a**	**D1**	**C1**	**C3**	**D1a**
Great Barrier Reef	10	86	100	9	56	208	239	34
Phuket	56	14	102	55	238	57	325	232
Western Indian	17	34	78	15	64	100	218	61
Western Caribbean	4	7	16	4	17	16	40	17
Florida	6	3	11	6	29	11	33	29

Interestingly, the Florida and Western Caribbean networks—where the observed symbionts exhibited the lowest node degrees and the lowest sums of degrees of their neighboring nodes (see Table 4.7)—still managed to reach a higher population size than the other networks in certain scenarios (Figs. 4.8(a)4.8(b),4.8(c)4.8(d),4.8(g) and 4.8(h)), including symbionts that had lower thermal tolerance. This outcome corroborates what was found in the results of the correlation analysis, which suggested a negative relationship between node degree and population growth.

It is also important to note that the larger networks, such as the Great Barrier Reef and Phuket, where the observed symbionts displayed higher node degrees and higher neighbor degree sums, tended to have a faster population decay than other networks (Figs. 4.8(b),4.8(f) and 4.8(h)). This trend suggests that nodes with fewer links have greater resilience to environmental stressors; yet it is also important to highlight that connectivity alone does not fully explain the observed patterns.

Moreover, it is worth noting that despite the varying patterns of network connectivity and environmental conditions, all observed symbiont populations exhibited declining population sizes over time. This consistent downward trend underscores the overall vulnerability of symbionts to thermal stress, highlighting that even in networks where some structural advantages might exist, the long-term survival of these species remains threatened.

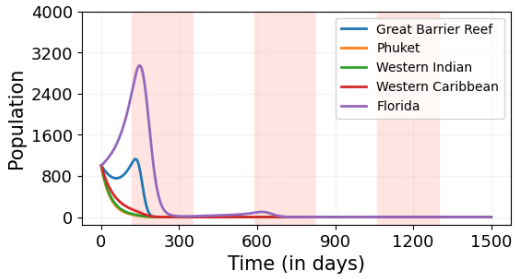

(a) Symbiont type D1 across different regions in linear scale

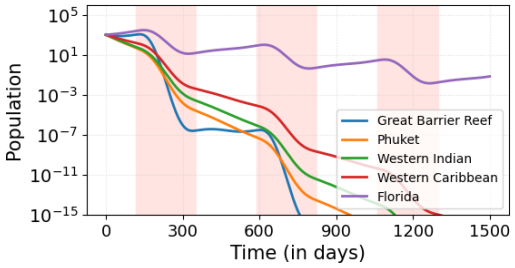

(b) Symbiont type D1 across different regions in semi-log scale

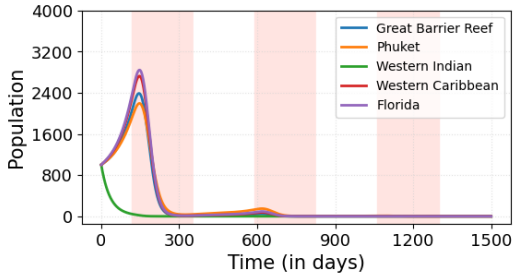

(c) Symbiont type C1 across different regions in linear scale

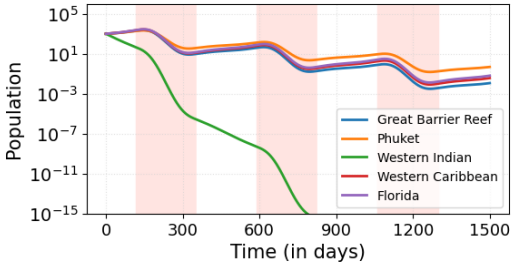

(d) Symbiont type C1 across different regions in semi-log scale

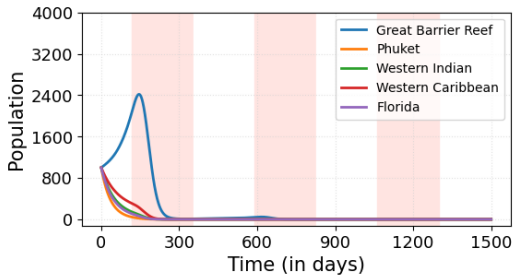

(e) Symbiont type C3 across different regions in linear scale

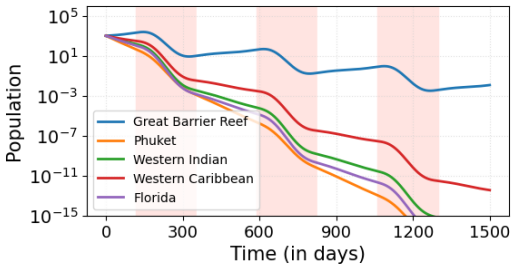

(f) Symbiont type C3 across different regions in semi-log scale

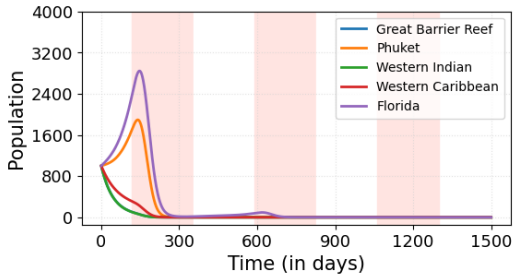

(g) Symbiont type D1a across different regions in linear scale

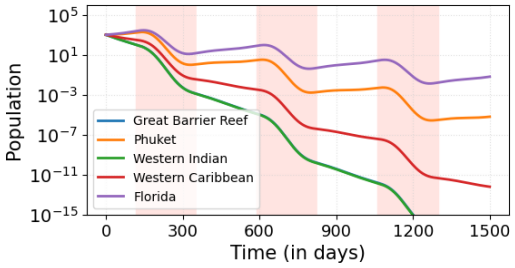

(h) Symbiont type D1a across different regions in semi-log scale

Figure 4.8: Comparison between the population dynamics of four different types of symbionts (D1, C1, C3 and D1a) that appeared in all regions analyzed.

Table 4.8: Structural characteristics (node degree and sum of neighbor degrees) of the same species of hosts that were found in different regions (Fig. 4.9). Thermal tolerance values for these types are *Pocillopora damicornis* (P.d.): 0.577, *Acropora tenuis* (A.t.): 0.622 and *Acropora valida* (A.v.): 0.837.

	Node degree			**Sum of neighbors' degree**		
Host species	**P.d.**	**A.t.**	**A.v.**	**P.d.**	**A.t.**	**A.v.**
Great Barrier Reef	8	3	1	101	191	100
Phuket	3	4	6	128	239	350
Western Indian	2	2	4	38	95	98
Florida	5	1	1	17	4	11

For the hosts, a similar overall declining trend in population dynamics was observed. However, two noteworthy cases emerged: the host species *Acropora tenuis* and *Acropora valida*. Specifically, *Acropora tenuis* demonstrated significantly higher population sizes in the Florida network compared to other regions (see Figs. 4.9(a), 4.9(c) and 4.9(e)). The case of *Acropora tenuis* is particularly interesting, as its population size managed to escape the overall declining trend and exhibited growth over time (see Fig. 4.9(d)). Moreover, *Acropora valida* in the West Indian region, it also managed to overcome this downward trend and reached considerable population sizes in this region, where it also has few links and its neighbors have few connections. These scenarios are especially relevant because they align with the expected relationship from the degree correlation analysis, indicating that species with fewer connections and less-connected neighbors can, in certain contexts, thrive even under stressful conditions.

Another important point concerns the connectivity patterns of the neighbors of these host species. It is evident that the neighbors of all three host species exhibited high degrees of connectivity, which is expected given the substantially higher number of hosts compared to symbionts in all networks, allowing symbionts to establish many connections. This high connectivity may significantly influence host population dynamics, as indicated by the negative correlation between neighbor degree and final population size: host growth tends to be constrained when neighboring symbionts are highly connected. This effect arises from the formulation in Eq.4.2, which shows that the contribution of each neighboring node to the growth of the target species decreases as the neighbor's degree increases.

These results, along with neighbor degree correlations, show that ecological network structure can positively or negatively affect population sizes, depending on context and local configuration—highlighting the complexity of such interactions.

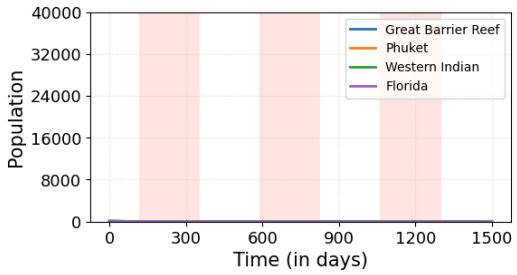

(a) Host species *Pocillopora damicornis* across different regions in linear scale

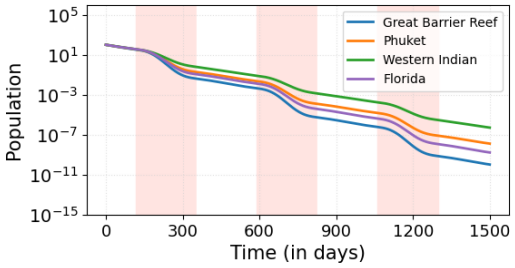

(b) Host species *Pocillopora damicornis* across different regions in semi-log scale

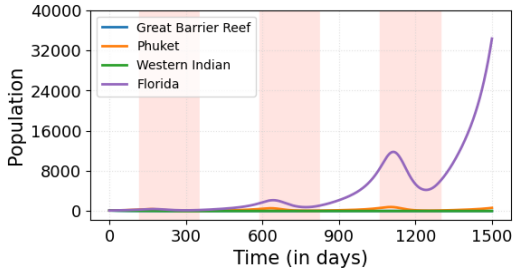

(c) Host species *Acropora tenuis* across different regions in linear scale

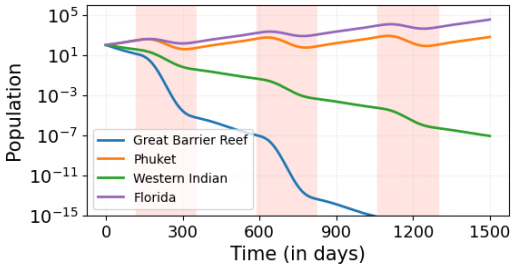

(d) Host species *Acropora tenuis* across different regions in semi-log

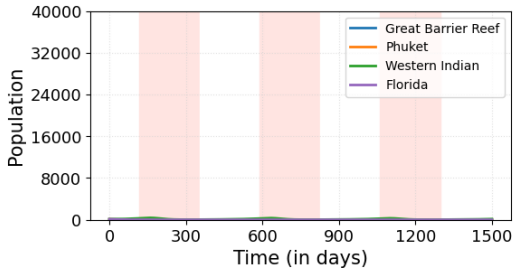

(e) Host species *Acropora valida* across different regions in linear scale

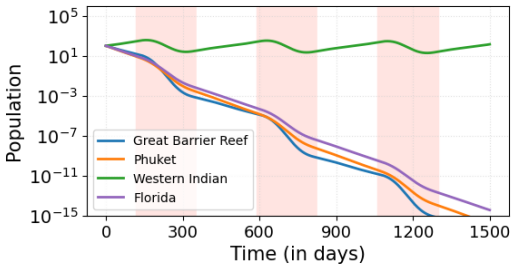

(f) Host species *Acropora valida* across different regions in semi-log scale

Figure 4.9: Comparison between the population dynamics of three different species of host (*Pocillopora damicornis*, *Acropora tenuis* and *Acropora valida*) that appeared in all regions analyzed, except Western Caribbean.

Chapter 5

Population Growth Model with Carrying Capacity

This chapter presents another model, the second proposed in this thesis, which includes a carrying capacity term that limits the growth of all species. Although it is a different model, this one also captures the population growth of the different species, taking into consideration the symbiotic network and water temperature variations.

5.1 Mathematical model

Essentially, the model is a system of coupled ordinary differential equations that tracks the dynamics of the symbiont population sizes over time. This model explicitly incorporates the network structure of the mutualistic relationship between symbionts and their host corals, where every node represents an organism's population size, and links represent the symbiotic interactions between the two types of organisms, exactly like the previous model. This model also uses a single variable per node instead of defining variables for each interaction (link). Consequently, this formulation greatly reduces the dimensionality of the system (see Table 3.1).

Let $S_i(t)$ denote the population size of symbiont i at time t. The population dynamics over time of S_i is given by:

$$\frac{dS_i}{dt} = \frac{\Delta_i^s}{K^s}\frac{S_i}{|N_i^s|}\left[K^s - S_i + \alpha_{sh}\left(\sum_{j\in N_i^s}\frac{H_j}{|N_j^h|}\right)\right] \tag{5.1}$$

Eq. 5.1 is inspired by the equations presented in the book KOT [19].

Table 5.1: Definition for symbols of variables and parameters of the model with carrying capacity.

Symbol	**Definition (variables and parameters)**
$S_i(t)$	population size of the i-th symbiont species at time t
$H_j(t)$	population size of the j-th host species at time t
N_i^s	neighborhood of the i-th symbiont species
N_j^h	neighborhood of the j-th host species
$\|N_i^s\|$	degree of the i-th symbiont species
$\|N_j^h\|$	degree of the j-th host species
r_i^s	growth rate of the i-th symbiont species
r_j^h	growth rate of the j-th host species
m_i^s	mortality rate of the i-th symbiont species
m_j^h	mortality rate of the j-th host species
Δ_i^s	net growth rate of the i-th symbiont species
Δ_j^h	net growth rate of the j-th host species
τ_i^s	thermal tolerance of the i-th symbiont species
τ_j^h	thermal tolerance of the j-th host species

Note that this equation combines both growth and network-driven interactions. The parameter Δ_i^s represents the net growth rate of symbiont i, defined as the difference between its intrinsic growth (r_i^s) and mortality rates (m_i^s). In this model, the intrinsic growth and mortality rates are also determined by Eqs. 4.4 and 4.5, respectively. This term captures the inherent biological capacity of the symbiont to increase its population size, reflecting both environmental conditions and species-specific characteristics independent of network interactions. Note that Δ_i^s can be positive or negative, depending on the balance between intrinsic growth and mortality processes. For example, a negative Δ_i^s implies that the symbiont cannot sustain itself without mutualistic support from host corals.

Figure 5.1 provides an intuitive view of how the net growth rate—defined as the difference between intrinsic growth (4.4) and mortality (4.5)—changes with temperature. As shown in the plot, when the system temperature rises above the optimal value, Δ_i^s becomes negative, indicating that mortality outweighs growth. In contrast, under cooling scenarios, the net growth rate remains positive. The figure also illustrates that organisms with higher thermal tolerance experience less severe reductions in net growth under warming conditions compared to those with lower thermal tolerance.

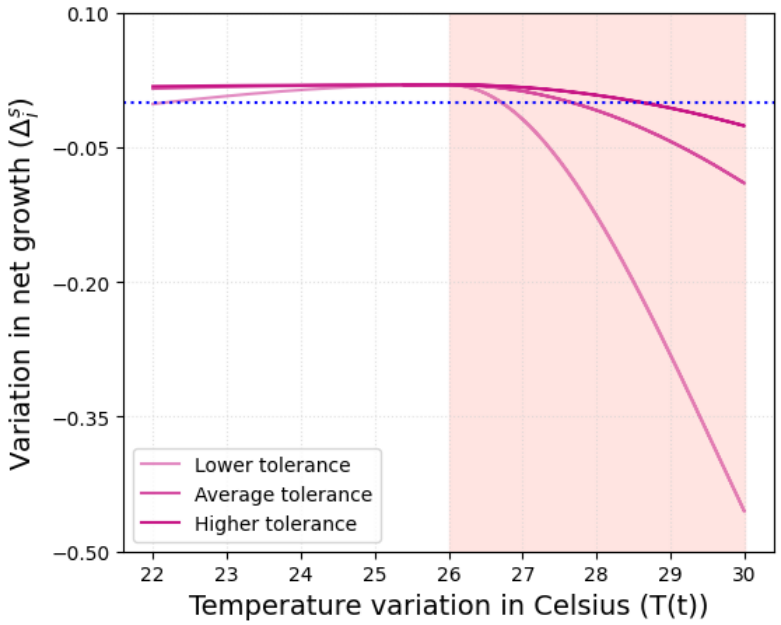

Figure 5.1: Variation in net growth of symbionts with different thermal tolerance values (τ_i^s) across different temperatures. The red zone in the plot mark when the system is above the optimal temperature for growth ($T(t) > z$) and the blue dotted line represents r_i^s and m_i^s equals to zero.

The net growth rate of symbiont i is given by:

$$\Delta_i^s = r_i^s - m_i^s \tag{5.2}$$

The parameter α_{sh} represents the strength of the mutualistic interaction between symbionts and hosts. A higher α_{sh} means that symbionts derive more substantial benefits from their interactions with hosts, increasing their population growth. This parameter thus controls the extent to which host population sizes can positively influence symbiont growth—a critical component of mutualistic networks.

The parameter α_{sh} represents the strength of the mutualistic interaction between symbionts and hosts. A higher α_{sh} means that symbionts derive more substantial benefits from their interactions with hosts, increasing their population growth. The value of α_{sh} is defined in the model as half of the maximum growth rate r_i^s (Eq. 4.4) of the symbiont. The maximum r_i^s is achieved when the system reaches the optimal temperature for growth—at this point ($T(t) = z$), the exponential term in the growth rate equation (see Eq. 4.4) becomes zero $\left(\frac{r_0^s}{\sqrt{2\pi}}.e^0\right)$, causing the entire exponential term to equal one, thereby maximizing r_i^s. This means that r_i^s attains its theoretical peak value under ideal thermal conditions (see Fig. 4.1(a)). Consequently, α_{sh} is defined as:

$$\alpha_{sh} = \frac{\frac{r_0^s}{\sqrt{2\pi}}}{2} \tag{5.3}$$

This definition ensures that the mutualistic contribution from the hosts cannot, by itself, exceed half of the maximum growth potential of the symbiont population. Biologically, this reflects the assumption that mutualistic interactions enhance—but do not completely determine—symbiont growth, which also depends on intrinsic and environmental factors.

In addition, it is important to highlight that the strength of the mutualistic interaction (α_{sh}) must be carefully constrained. According to the model derivation (see KOT [19] pg. 226), the product $\alpha_{sh}\alpha_{hs}$ must be less than one ($\alpha_{sh}\alpha_{hs} < 1$). Otherwise, the mutualistic benefit would overpower the density-dependent regulation ($K_s - S_i$), causing the system to diverge instead of stabilizing at an equilibrium. In other words, if α_{sh} is too large, the positive feedback from the mutualistic interaction could lead to uncontrolled exponential growth of the symbiont population — an unrealistic scenario that would not reflect natural population dynamics. Moreover, one key aspect of this model is the assumption that α_{sh} is always positive. This reflects the fundamental assumption that the mutualistic interaction between symbionts and hosts is always beneficial.

The term K_s denotes the carrying capacity of the symbiont population, set to 10^4 in this model. This parameter represents the maximum number of individuals that an environment can sustainably support. The logistic component $K_s - S_i$ captures intraspecific competition; when the symbiont population size S_i is small, the expression is positive, encouraging growth. As S_i approaches K_s, the term decreases, slowing the growth rate, ensuring that the population size saturates at the carrying capacity and cannot grow indefinitely. The additional term $\left(\alpha_{sh}\left(\sum_{j\in N_i^s}\frac{H_j}{|N_j^h|}\right)\right)$ in Eq. 5.1 represents the positive contribution of neighboring host population sizes to the growth of the symbiont, normalized by the connectivity ($|N_j^h|$) of those hosts. This term allows the model to capture the benefits of mutualism: the presence of neighboring host populations can enhance the growth rate of the symbionts.

Analyzing this model, it is possible to identify two key equilibrium points: extinction and coexistence. The extinction equilibrium occurs when $S_i^* = 0$, corresponding to the collapse of the symbiont population, which may occur in the absence of sufficient growth or mutualistic support. The coexistence equilibrium occurs when $S_i^* = K_s + \alpha_{sh}\left(\sum_{j\in N_i^s}\frac{H_j}{|N_j^h|}\right)$. This positive equilibrium represents a stable state in which the symbiont population size not only grows to fill the carrying capacity but also benefits from the positive influence of its host neighbors. The additional term proportional to α_{sh} highlights the important role of mutualism in enhancing the effective carrying capacity of the symbiont population.

Additionally, note that the term $\frac{S_i}{|N_i^s|}$ distributes the mutualistic benefits proportionally among the symbiont's neighbors. Dividing the population size of an organism by its degree assumes that each population interacts uniformly with the

population of neighboring organisms. This normalization ensures that the interaction of a symbiont or host population is distributed evenly among its connections, preventing highly connected symbionts from gaining an unrealistic advantage simply because they have more neighbors.

The population dynamics(derivative) of H_j over time is given by:

$$\frac{dH_j}{dt} = \frac{\Delta_j^h}{K^h}\frac{H_j}{|N_j^h|}\left[K^h - H_j + \alpha_{sh}\left(\sum_{i \in N_j^h}\frac{S_i}{|N_i^s|}\right)\right] \tag{5.4}$$

Note that this equation is identical to Eq. 5.1 making the model symmetric. The net growth rate, growth rate, mortality rate, and the positive force of mutualism are also given by equations Eq. 5.2, Eq. 4.4, Eq. 4.5 and Eq. 5.3, respectively (replacing superscript s with h and subscript i with j, as shown in Table 5.2). Therefore, there is no inherent population growth advantage between symbionts and hosts. Of course, in this model, their growth also depends on the parameters of the model such as network structure, thermal tolerance, water temperature, and initial population sizes.

Table 5.2: Parameter definitions and values used in the numerical evaluation.

Parameter	**Value**	**Definition**
r_0^s	0.25	scaling factor for symbionts' growth rate
r_0^h	0.25	scaling factor for hosts' growth rate
z	26°C	optimum growth temperature for symbionts and hosts
μ	0.08	the base mortality rate
γ_r	$8 \cdot 10^{-4}$	damping coefficient for growth
γ_m	$2 \cdot 10^{-3}$	damping coefficient for mortality
K_s	10^4	carrying capacity of symbionts
K_h	10^3	carrying capacity of hosts
α_{sh}	0.099	positive effective of host on symbionts
α_{hs}	0.099	positive effective of symbionts on hosts

The parameters r_0^s and r_0^h were used in the MCMANUS *et al.* [37] article with values equal to 1. Furthermore, the base mortality was used in MCMANUS *et al.* [37] with a value equal to zero and used in WALSWORTH *et al.* [40] with a value equal to 0.1.

The net growth depends on the growth rate (Eq. 4.4) and mortality rate (Eq. 4.5) of symbionts and hosts, which depend on the current local sea temperature. Thus, a model for the variation of the sea temperature is needed. The water temperature model is identical to the one used in the first model presented in Chapter 4 (see Eq.

4.7).

The choice of parameters for the temperature model was arbitrary to emulate recurrence within a temperature range and timescale.

Finally, Eq. 5.1 and Eq. 5.4 will be solved numerically and independently for each region (see Table 3.1) according to the temperature model (Eq. 4.7) over a time horizon that simulates successive warming events over 4500 days.

5.2 Results

Similar to what was done in the first model, numerical analysis of these coupled dynamics were performed, so that it is possible to explore not only how individual species behave, but also how the structure of the network shapes the overall population trajectories over time. This approach allows us to investigate how the structure of the network influences the resilience and recovery of these populations after heat stress events.

To investigate how network structure influences population dynamics, all species were initialized with non-zero population sizes: each symbiont started with 1,000 individuals, and each host species with 100. This standardized initialization ensures that no species has an initial advantage, allowing any differences in population trajectories over time to be attributed to the network structure and model dynamics, rather than unequal starting conditions. The coupled differential equations governing symbiont and host populations sizes over time (Eqs. 5.1–5.4) were solved numerically for each region using Python's `scipy.integrate.odeint` function. All model parameters were kept identical across regions, ensuring that observed differences in population growth or decline result solely from network topology and initial conditions. The full implementation—including data preprocessing, parameter definitions, and the use of `odeint`—is available here.

5.2.1 Population Dynamics

Unlike what was observed with the model presented in the previous section, in the current model incorporating carrying capacity, the populations demonstrated an improved ability to thrive. For example, considering the symbiont populations that previously exhibited a pronounced decay trend (as shown in Fig. 4.3), more symbiont species now successfully converge towards the carrying capacity of the model, although they converge at different rates. This indicates that the carrying capacity allows for a more stable population dynamic compared to the earlier model.

Despite the improved stability introduced by the carrying capacity, it is evident that some symbiont populations continue to converge towards the extinction equi-

librium point (see Figs. 5.2 and 5.3 and Table 5.3). This outcome suggests that while the carrying capacity supports population persistence for some nodes, certain local interactions or initial conditions may still drive specific populations towards extinction. Consequently, the carrying capacity acts as a regulatory mechanism that balances population growth but does not guarantee universal survival.

Regarding host populations, a pattern of improved resilience is observed when compared to the numerical results in Fig. 4.4. However, hosts now (Fig. 5.3) show a more pronounced ability to thrive, with most populations achieving steady growth over time. Furthermore, an interesting difference can be noted when comparing the dynamics of hosts and symbionts. As illustrated in Figs. 5.2 and 5.3, more host species can reach population equilibrium at carrying capacity and they converge more quickly to this equilibrium than symbionts. This observation indicates that hosts are more efficient in reaching their carrying capacity.

Moreover, across all scenarios analyzed, hosts exhibit a lower proportion of populations that converge towards the extinction equilibrium compared to symbionts (see Table 5.3). This pattern underscores the differential resilience of the two groups and highlights the asymmetric nature of the interactions modeled within this framework. One possible explanation for this difference lies in the structure of the network itself: hosts typically have fewer neighbors than symbionts. Additionally, the interaction term involving hosts and symbionts might be configured in such a way that hosts benefit more consistently from mutualistic interactions, thereby enhancing their growth potential.

Finally, when comparing the results presented in Table 4.3 with those in Table 5.3, a clear difference emerges regarding species persistence between the two models. In the second model, the percentage of species that went extinct—defined here as populations that converged to zero over the course of the simulation—is substantially lower than in the first. This trend holds across both groups of organisms, but is especially pronounced for host species, which show a marked increase in survival rates under the second modeling approach. Furthermore, in both models, host species showed lower extinction rates than symbionts, indicating more robust population dynamics in this group. Here, robust refers to a comparatively better population outcome: although population sizes in these networks still declined under thermal stress, the decline occurred more slowly or less severely than in others.

Overall, these results emphasize the crucial role that carrying capacity plays in shaping the long-term dynamics of the model. By imposing an upper bound on population size (which does not happen in the previous model, as you may see in Figs. 4.3 and 4.4), the carrying capacity acts as a stabilizing force that mitigates unbounded growth and provides a mechanism for population sizes to reach a stable equilibrium. Furthermore, the differences in convergence rates between hosts and

symbionts highlight the importance of accounting for the network structure and local interactions when interpreting the trajectories of these populations.

Table 5.3: Percentage of species that became extinct over the course of population dynamics in the different regions.

Region	**Symbiont species**	**Host species**
Great Barrier Reef	86.8%	21.7%
Phuket	75.0%	25.6%
Western Indian	79.1%	20.6%
Western Caribbean	83.3%	0%
Florida	76.9%	12.5%

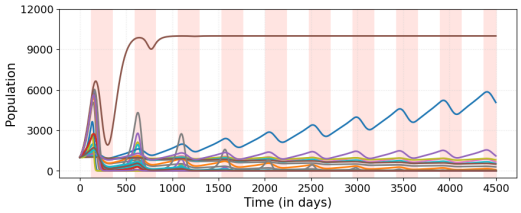

(a) Symbionts at Great Barrier Reef in linear scale

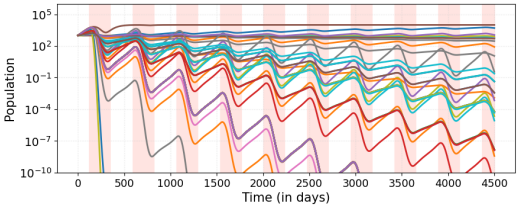

(b) Symbionts at Great Barrier Reef in semi-log scale

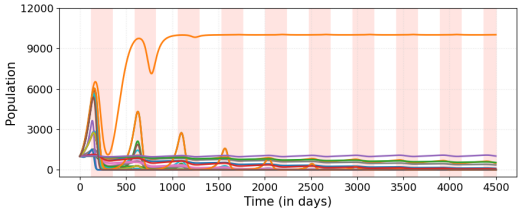

(c) Symbionts at Phuket in linear scale

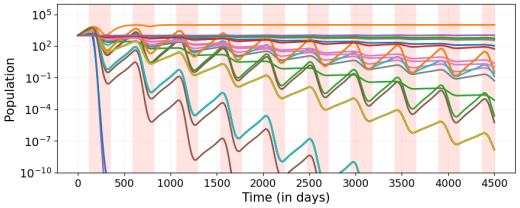

(d) Symbionts at Phuket in semi-log scale

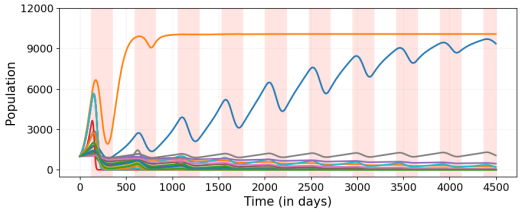

(e) Symbionts at Western Indian in linear scale

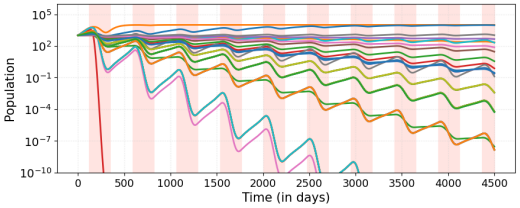

(f) Symbionts at Western Indian in semi-log scale

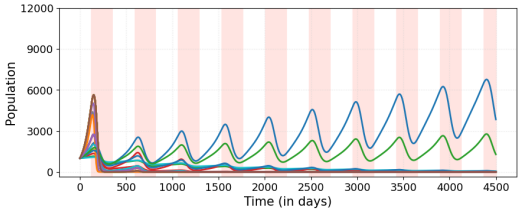

(g) Symbionts at Western Caribbean in linear scale

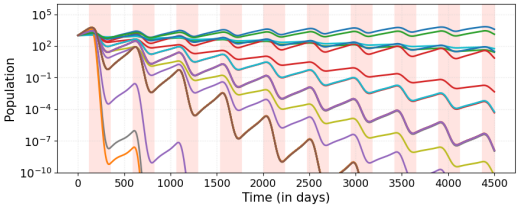

(h) Symbionts at Western Caribbean in semi-log scale

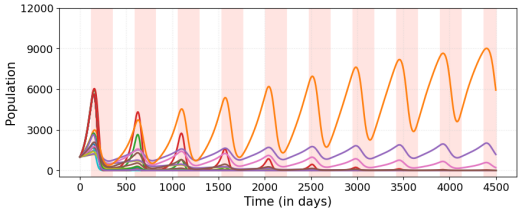

(i) Symbionts at Florida in linear scale

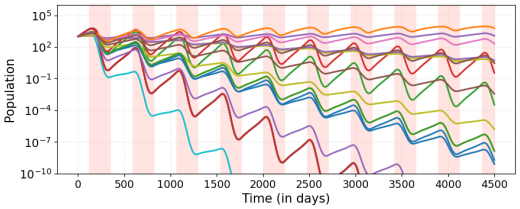

(j) Symbionts at Florida in semi-log scale

Figure 5.2: Population dynamics of symbiont species in the five regions studied (Table 3.1). On the left, linear scale plots with identical y-axis ranges facilitate comparisons across regions. On the right, semi-log plots (logarithmic y-axis) reveal different population size magnitudes over time. Red colored zones mark when the environment is heating up($T(t)) > z$).

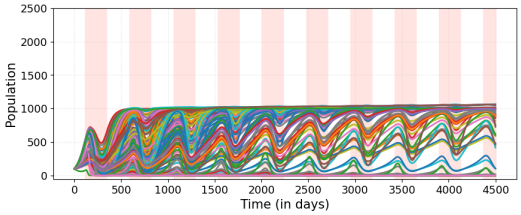

(a) Hosts at Great Barrier Reef in linear scale

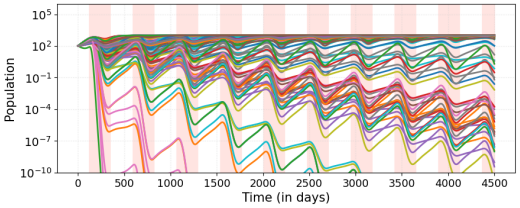

(b) Hosts at Great Barrier Reef in semi-log scale

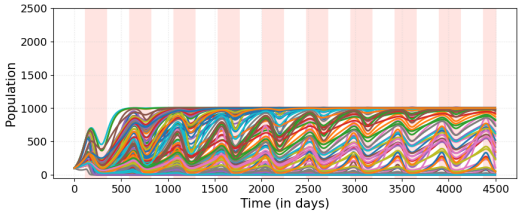

(c) Hosts at Phuket in linear scale

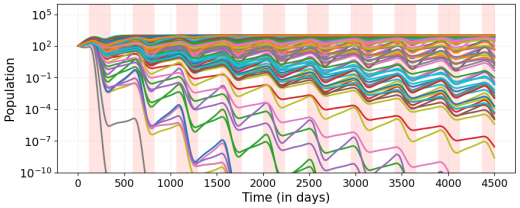

(d) Hosts at Phuket in semi-log scale

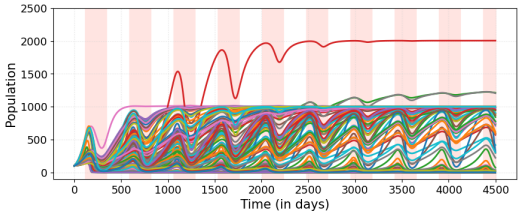

(e) Hosts at Western Indian in linear scale

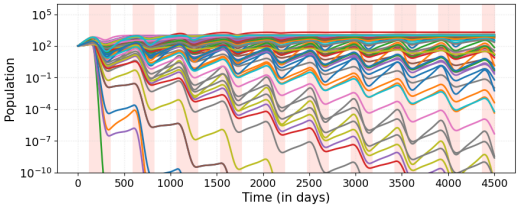

(f) Hosts at Western Indian in semi-log scale

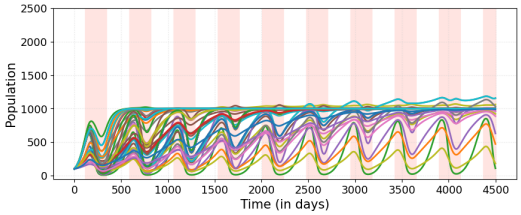

(g) Hosts at Western Caribbean in linear scale

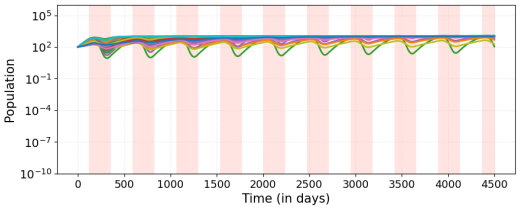

(h) Hosts at Western Caribbean in semi-log scale

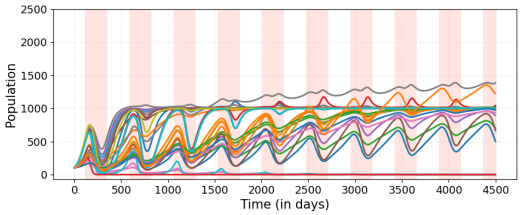

(i) Hosts at Florida in linear scale

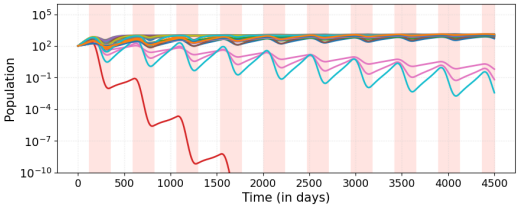

(j) Hosts at Florida in semi-log scale

Figure 5.3: Population dynamics of host species in the five regions studied (Table 3.1). On the left, linear scale plots with identical y-axis ranges facilitate comparisons across regions. On the right, semi-log plots (logarithmic y-axis) reveal different population size magnitudes over time. Red colored zones mark when the environment is heating up $(T(t)) > z$).

Fig. 5.4 presents the complementary cumulative distribution functions of the final population sizes (i.e., at time $t = 4500$) of both symbionts and hosts.

For symbionts (Fig.5.4(a)), the results clearly indicate that most species experienced population decline to the point of extinction, with their sizes converging to zero by the end of the simulation. Only a very small fraction of symbiont species managed to persist and reach their carrying capacity equilibrium, highlighting the overall fragility of this group under the modeled conditions. In contrast, host species exhibited a markedly different pattern, as shown in Fig.5.4(b). A substantial proportion of host populations successfully converged to their carrying capacity, suggesting greater stability and resilience. This is especially evident in the Western Caribbean region, where all host species reached the carrying capacity equilibrium, indicating complete survival across the network in that area. These contrasting outcomes emphasize the distinct dynamics and vulnerabilities of hosts and symbionts within the same ecological framework.

Overall, these results reinforce the role of carrying capacity as a stabilizing factor in the system and highlight differences in the dynamics of symbiont and host populations. The complementary cumulative distribution functions thus provide a clear way to compare the convergence behavior of both groups in the network.

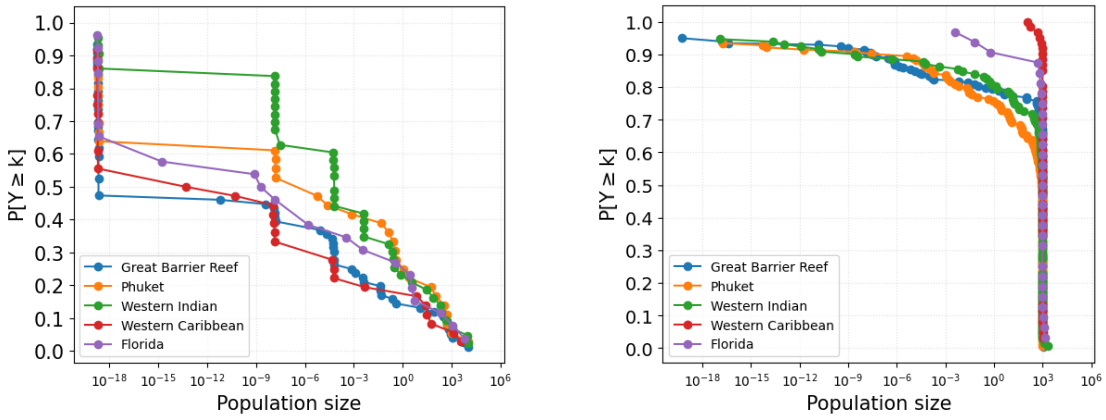

(a) Distribution of symbiont population sizes

(b) Distribution of host population sizes

Figure 5.4: Complementary cumulative distribution function of symbionts' (left) and hosts' (right) final population sizes in their respective collection region.

5.2.2 Influence of Network Structure

The role of network structure and species' thermal tolerances in shaping population size outcomes can also be studied through correlation analysis. By assessing the relationship between these factors and the final population sizes achieved by each species, we can better understand how both intrinsic traits and network connectiv-

ity influence species' resilience. In all cases, these relationships are quantified using Pearson correlation coefficients.

Table 5.4 presents the correlation coefficients between thermal tolerance and final population size (at time $t = 4500$) across all regions. Similar to the correlation analysis done in Table 4.4, these correlations are consistently high, indicating that species with greater thermal tolerance tend to achieve larger final population sizes after the numerical analysis. To ensure a fair analysis, the correlation was calculated between the logarithm of the population sizes (at time $t = 4500$), rather than the raw population sizes. This transformation compresses the scale of the data and helps balance the differences in magnitude between the population sizes and the thermal tolerance values (which range between 0 and 1). Without this transformation, the magnitude of the population size data could have dominated the correlation calculation, potentially overshadowing the role of thermal tolerance in driving population growth.

Table 5.4: Correlation between final population sizes and thermal tolerances in the different regions.

Region	**Symbiont nodes**	**Host nodes**
Great Barrier Reef	0.712	0.648
Phuket	0.635	0.663
Western Indian	0.502	0.653
Western Caribbean	0.781	0.269
Florida	0.643	0.652

In the previous section, Table 4.5 presents the correlation between the population size at time $t = 830$ of species and their node degrees across different regions, showing that for most regions, the correlation values are below -0.3 (which is generally considered a moderate negative correlation) for both symbionts and hosts. However, this pattern is not observed in Table 5.5.

As shown, neither the symbionts (with the exception of those in Florida) nor the host species exhibited significant correlations between node degree and final population size. In the case of host species, correlation values were consistently close to zero, indicating a complete absence of correlation. These results suggest that, under the second model, the number of neighbors a species has in the network does not play a major role in determining its population outcome. In other words, network connectivity alone appears to have a much weaker influence on population dynamics when compared to the first model, possibly due to the presence of additional regulatory mechanisms such as carrying capacity or intrinsic biological thresholds.

Table 5.5: Correlation between final population sizes and node degrees in the different regions.

Region	Symbiont nodes	Host nodes
Great Barrier Reef	0.173	0.030
Phuket	0.252	0.016
Western Indian	0.192	0.149
Western Caribbean	0.298	-0.057
Florida	0.512	0.036

Finally, Table 5.6 shows the correlation between the sum of the degrees of each species' neighbors and their final population sizes. In contrast to the results presented in Tables 4.5 and 4.6, symbionts displayed positive correlations in this case—although the values were not statistically significant. This suggests a weak tendency for symbionts connected to highly connected species to reach slightly higher population sizes, but without consistent or meaningful strength. For host species, the same pattern observed in Table 5.5 was repeated: there was no clear correlation between the sum of neighbor degrees and final population sizes. These findings further support the idea that, in the second model, local connectivity—whether measured directly through degree or indirectly through neighbor influence—has limited explanatory power over the population dynamics of both groups, especially hosts.

Table 5.6: Correlation between final population sizes and sum of degrees of neighbors in the different regions.

Region	Symbiont nodes	Host nodes
Great Barrier Reef	0.171	-0.074
Phuket	0.256	-0.038
Western Indian	0.205	0.068
Western Caribbean	0.299	-0.075
Florida	0.424	0.055

In addition to the correlation analyses, plots to visually illustrate how the population dynamics of both symbionts and hosts unfold across the networks were made. These plots help to understand how network structure influences species' resilience in a more intuitive way.

The networks analyzed share several symbiont and host species in common, but to focus the analysis and maintain consistency, four symbiont types (D1, C1, C3 and D1a) that are present in all networks and three host species (*Pocillopora damicornis*, *Acropora tenuis* and *Acropora valida*) that are present in all region networks, except

Western Caribbean, were selected to be analyzed. These selected symbionts and host species were exposed to the same thermal variation conditions across all networks, ensuring that any differences observed are not due to differences in environmental stress. Moreover, each symbiont's and host's thermal tolerance—a fixed, species-specific trait—remained constant regardless of the region in which the organism was found. Thus, the only factor that varied among the networks was the structure of interactions, which was measured using metrics such as node degree and sum of neighbors' degree.

As detailed in the Tables 4.7 4.8, these symbiont types and hosts species exhibits different degrees and sum of neighbors' degree depending on the network. These structural differences affect how each species interacts with others and, ultimately, how its population grows or declines over time.

Hence, Figs. 5.5 and 5.6demonstrate how the population dynamics of both symbionts and hosts change when the degree and the sum of the degrees of their neighbors differ from one network to another. This approach assess how variations in network structure—independent of species traits like thermal tolerance—shape population trajectories and potentially influence community resilience under repeated thermal stress events.

As shown in Fig. 5.5, symbiont populations in nearly all regions tended to decline and eventually converge to zero, reflecting a general vulnerability of these organisms under the modeled conditions. However, in some regions—particularly where symbionts had a greater number of connections and were linked to neighbors that were themselves highly connected—this decline was delayed. In a few notable cases, these structural advantages even allowed the symbionts to increase their populations over time. A clear example of this is symbiont D1 in the Phuket region, which not only avoided extinction but exhibited population growth throughout the simulation (see Fig. 5.5(b)).

This behavior may be related to the weak but positive correlations observed between population size and both node degree and neighbor degree sum, as reported in Tables 5.5 and 5.6. Although these correlations are not statistically strong, they suggest that local connectivity and indirect structural support from neighboring species can influence the persistence and success of certain symbionts within the network, especially under environmental stress.

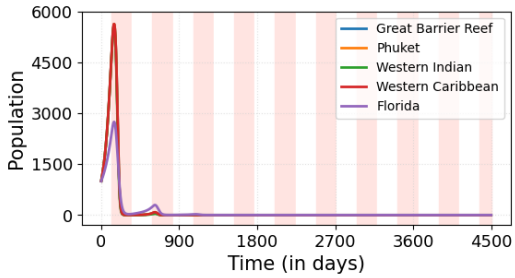

(a) Symbiont type D1 across different regions in linear scale

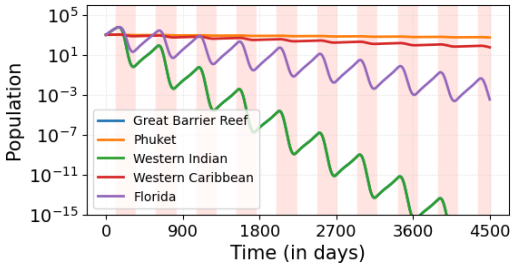

(b) Symbiont type D1 across different regions in semi-log scale

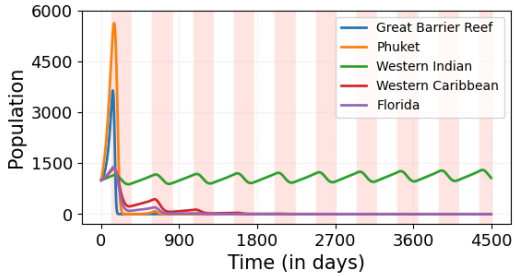

(c) Symbiont type C1 across different regions in linear scale

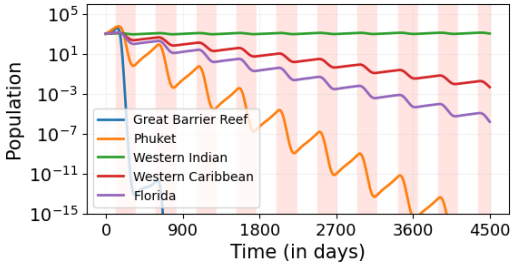

(d) Symbiont type C1 across different regions in semi-log scale

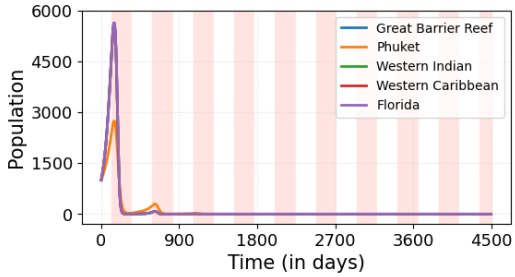

(e) Symbiont type C3 across different regions in linear scale

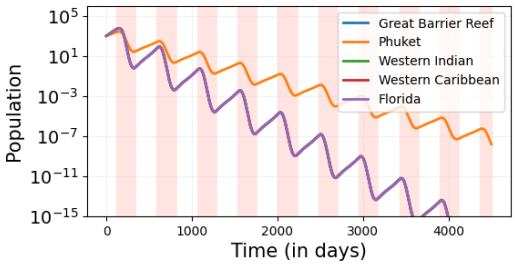

(f) Symbiont type C3 across different regions in semi-log scale

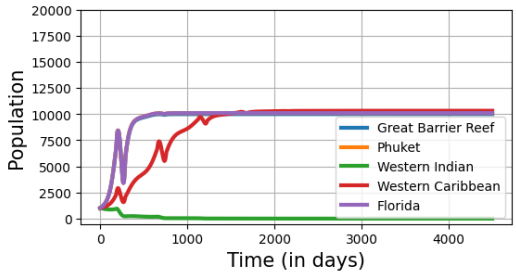

(g) Symbiont type D1a across different regions in linear scale

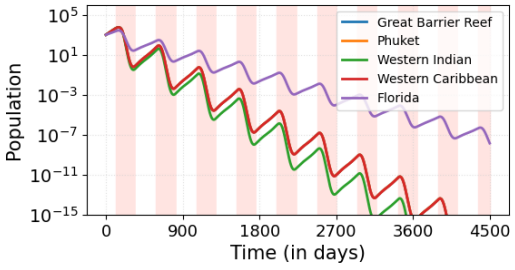

(h) Symbiont type D1a across different regions in semi-log scale

Figure 5.5: Comparison between the population dynamics of four different types of symbionts (D1, C1, C3 and D1a) that appeared in all regions analyzed.

For host populations, an interesting and somewhat unexpected pattern emerged. Although the correlation analyses in Tables 5.5 and 5.6 indicated no significant relationship between final population size and either node degree or the sum of neighbors' degrees, Fig. 5.6 reveals a distinct outcome in the Florida region. In all scenarios, host species (with different thermal tolerance values) in this region consistently achieved higher population sizes by the end of the simulation. This is particularly notable given that the Florida network is characterized by relatively low degrees and weak neighbor connectivity. Despite these structural limitations, the same host species—when embedded in larger or more connected networks—displayed poorer population performance.

Furthermore, these analyses emphasize the importance of local network structure in determining the population dynamics of symbionts and highlight how the interplay between network structure and biological parameters can affect the overall resilience and persistence of coral–algal systems.

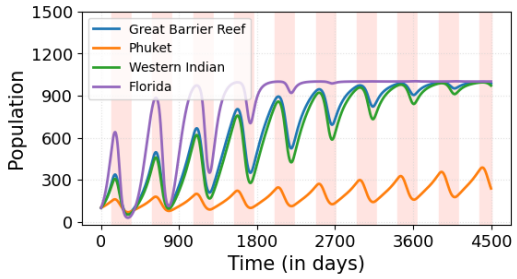

(a) Host species *Pocillopora damicornis* across different regions in linear scale

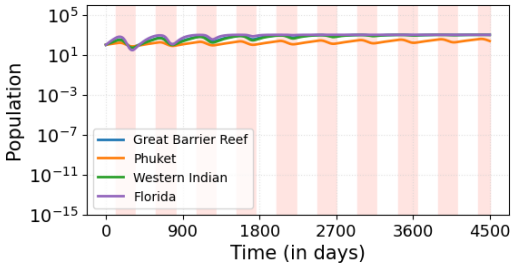

(b) Host species *Pocillopora damicornis* across different regions in semi-log scale

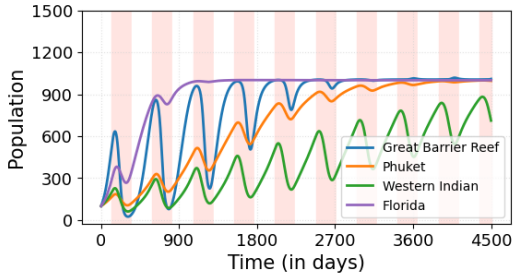

(c) Host species *Acropora tenuis* across different regions in linear scale

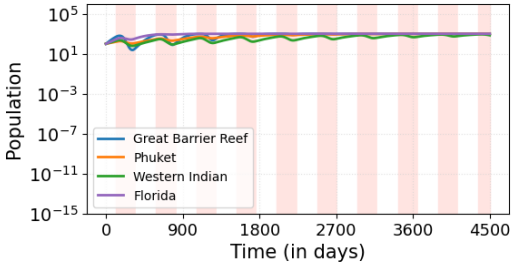

(d) Host species *Acropora tenuis* across different regions in semi-log

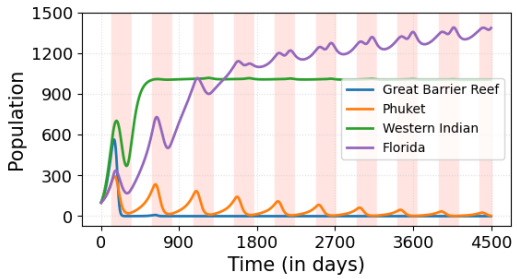

(e) Host species *Acropora valida* across different regions in linear scale

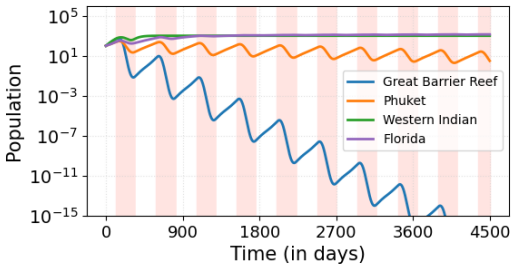

(f) Host species *Acropora valida* across different regions in semi-log scale

Figure 5.6: Comparison between the population dynamics of three different species of host (*Pocillopora damicornis*, *Acropora tenuis* and *Acropora valida*) that appeared in all regions analyzed, except Western Caribbean.

Chapter 6

Conclusions

In this study, the interplay between network structure and population dynamics in the global coral–symbiont network under varying water temperatures was systematically analyzed through the development and implementation of two mathematical models. The first model captures population dynamics without an upper limit on growth, while the second introduces a carrying capacity that restricts population growth, providing a more biologically realistic scenario. These models, offer insights into how different network structures and species-specific traits modulate the resilience of coral–algal systems in the face of repeated warming events.

The analysis revealed that even when all species begin with identical initial population sizes and parameter values, differences in population trajectories emerge due to the structure of the network and species-specific thermal tolerances. Symbionts in particular exhibited a pronounced decline in the first model, highlighting their vulnerability to repeated thermal stress events. However, the carrying capacity model allowed some symbiont species to stabilize near the carrying capacity, even though some populations still converged to extinction points depending on local interactions and initial conditions.

Host populations demonstrated greater resilience compared to their symbiotic partners in both models. This result aligns with their generally higher thermal tolerance values and lower network connectivity, which reduces their exposure to negative indirect effects from neighboring symbiont collapses. Interestingly, the structure of the symbiotic network proved to be a key factor in shaping the population trajectories of both hosts and symbionts.

The complementary cumulative distribution functions of population sizes further emphasized the role of network structure. While heavy-tailed distributions were observed in real networks—particularly for host populations—randomized networks generally exhibited lighter tails, indicating reduced resilience and stability when biological symbiotic affinities are disrupted. These findings highlight the importance of preserving the ecological network structure to maintain the resilience of coral reef

ecosystems.

Moreover, correlation analyses revealed complex relationships between node degrees, sum of neighbor degrees, and final population sizes. Contrary to the initial hypothesis suggested by degree correlations, higher connectivity did not always translate into better population performance. For symbionts, negative correlations were often observed, indicating that species with fewer direct connections were better able to thrive under thermal stress. In contrast, host population sizes sometimes exhibited zero correlation between degree and population size.

Altogether, these results demonstrate that resilience in coral–algal systems is not determined solely by individual species traits or environmental factors, but is fundamentally shaped by the structure of their interaction network. This finding underscores the importance of considering network structure in conservation strategies to enhance reef resilience in the face of climate change.

6.1 Future Work

The present study helps to understand the dynamics of coral-symbiont interactions under changing environmental conditions. However, there are several promising avenues for extending this research in the future.

First, incorporating additional ecological processes such as competition, predation, or evolutionary dynamics could provide a more reliable model. These processes often interact with mutualistic relationships in complex ways, and their inclusion may reveal emergent patterns or thresholds not captured by the current model.

Second, future work could involve utilizing empirical databases on population growth or coral bleaching that account for both network structure and temperature variability. Integrating such datasets would enable the calibration and validation of the model under real-world scenarios, enhancing its predictive power and relevance to conservation efforts.

Lastly, biological validation of the model could be pursued through collaboration with experts in marine ecology. These specialists could interpret the numerical results within a biological context, ensuring that model outputs align with observed ecological phenomena and providing valuable feedback for refining the model's assumptions and parameters.

These proposed directions represent important steps towards developing a robust framework for understanding the complex dynamics of coral reef ecosystems under environmental stressors.

References

[1] "XL Catlin Seaview Survey". `https://www.catlinseaviewsurvey.com/coral-bleaching`. Accessed: 2025-05-23.

[2] DONNER, S. D., SKIRVING, W. J., LITTLE, C. M., et al. "Global assessment of coral bleaching and required rates of adaptation under climate change", *Global Change Biology*, v. 11, n. 12, pp. 2251–2265, 2005.

[3] WILLIAMS, S. D., PATTERSON, M. R. "Resistance and robustness of the global coral–symbiont network", *Ecology*, v. 101, n. 5, 2020.

[4] HUGHES, T. P., KERRY, J. T., BAIRD, A. H., et al. "Global warming transforms coral reef assemblages", *Nature*, v. 556, n. 7702, pp. 492–496, 2018.

[5] SWAIN, T. D., CHANDLER, J., BACKMAN, V., et al. "Consensus thermotolerance ranking for 110 Symbiodinium phylotypes: an exemplar utilization of a novel iterative partial-rank aggregation tool with broad application potential", *Functional Ecology*, v. 31, n. 1, pp. 172–183, 2017.

[6] ROWAN, R., KNOWLTON, N., BAKER, A., et al. "Landscape ecology of algal symbionts creates variation in episodes of coral bleaching", *Nature*, v. 388, n. 6639, pp. 265–269, 1997.

[7] GLYNN, P. W., MATÉ, J. L., BAKER, A. C., et al. "Coral bleaching and mortality in Panama and Ecuador during the 1997–1998 El Niño–Southern Oscillation event: spatial/temporal patterns and comparisons with the 1982–1983 event", *Bulletin of Marine Science*, v. 69, n. 1, pp. 79–109, 2001.

[8] TOLLER, W. W., ROWAN, R., KNOWLTON, N. "Repopulation of zooxanthellae in the Caribbean corals Montastraea annularis and M. faveolata following experimental and disease-associated bleaching", *The Biological Bulletin*, v. 201, n. 3, pp. 360–373, 2001.

[9] BUDDEMEIER, R. W., FAUTIN, D. G. "Coral bleaching as an adaptive mechanism", *Bioscience*, v. 43, n. 5, pp. 320–326, 1993.

[10] WEIS, V. M., REYNOLDS, W. S., DEBOER, M. D., et al. "Host-symbiont specificity during onset of symbiosis between the dinoflagellates Symbiodinium spp. and planula larvae of the scleractinian coral Fungia scutaria", *Coral reefs*, v. 20, pp. 301–308, 2001.

[11] JONES, A., BERKELMANS, R. "Potential costs of acclimatization to a warmer climate: growth of a reef coral with heat tolerant vs. sensitive symbiont types", *PloS one*, v. 5, n. 5, pp. e10437, 2010.

[12] LITTLE, A. F., VAN OPPEN, M. J., WILLIS, B. L. "Flexibility in algal endosymbioses shapes growth in reef corals", *Science*, v. 304, n. 5676, pp. 1492–1494, 2004.

[13] VERHULST, P.-F. "Notice sur la loi que la population suit dans son accroissement", *Correspondence mathematique et physique*, v. 10, pp. 113–129, 1838.

[14] PEARL, R., REED, L. J. "On the rate of growth of the population of the United States since 1790 and its mathematical representation", *Proceedings of the national academy of sciences*, v. 6, n. 6, pp. 275–288, 1920.

[15] SMITH, F. E. "Population dynamics in Daphnia magna and a new model for population growth", *Ecology*, v. 44, n. 4, pp. 651–663, 1963.

[16] LOTKA, A. J. "Analytical note on certain rhythmic relations in organic systems", *Proceedings of the National Academy of Sciences*, v. 6, n. 7, pp. 410–415, 1920.

[17] LOTKA, A. J. *Elements of physical biology*. Williams & Wilkins, 1925.

[18] ROSENZWEIG, M. L., MACARTHUR, R. H. "Graphical representation and stability conditions of predator-prey interactions", *The American Naturalist*, v. 97, n. 895, pp. 209–223, 1963.

[19] KOT, M. *Elements of Mathematical Ecology*. Cambridge University Press, 2001.

[20] MURRAY, J. D. *Mathematical biology: I. An introduction*, v. 17. Springer Science & Business Media, 2007.

[21] HOLLAND, J. N., DEANGELIS, D. L. "A consumer–resource approach to the density-dependent population dynamics of mutualism", *Ecology*, v. 91, n. 5, pp. 1286–1295, 2010.

[22] BASTOLLA, U., FORTUNA, M. A., PASCUAL-GARCÍA, A., et al. "The architecture of mutualistic networks minimizes competition and increases biodiversity", *Nature*, v. 458, n. 7241, pp. 1018–1020, 2009.

[23] VERBOOM, J., SCHIPPERS, P., CORMONT, A., et al. "Population dynamics under increasing environmental variability: implications of climate change for ecological network design criteria", *Landscape ecology*, v. 25, pp. 1289–1298, 2010.

[24] BARY, A. D. "Die Erscheinung der Symbiose. Karl J. Trübner, Strassburg". 1879.

[25] RELMAN, D. A. "'Til death do us part': coming to terms with symbiotic relationships." *Nature Reviews Microbiology*, v. 6, n. 10, 2008.

[26] DUBILIER, N., BERGIN, C., LOTT, C. "Symbiotic diversity in marine animals: the art of harnessing chemosynthesis", *Nature Reviews Microbiology*, v. 6, n. 10, pp. 725–740, 2008.

[27] DETHLEFSEN, L., MCFALL-NGAI, M., RELMAN, D. A. "An ecological and evolutionary perspective on human–microbe mutualism and disease", *Nature*, v. 449, n. 7164, pp. 811–818, 2007.

[28] LEY, R. E., LOZUPONE, C. A., HAMADY, M., et al. "Worlds within worlds: evolution of the vertebrate gut microbiota", *Nature Reviews Microbiology*, v. 6, n. 10, pp. 776–788, 2008.

[29] WERREN, J. H., BALDO, L., CLARK, M. E. "Wolbachia: master manipulators of invertebrate biology", *Nature Reviews Microbiology*, v. 6, n. 10, pp. 741–751, 2008.

[30] MUSCATINE, L., PORTER, J. W. "Reef corals: mutualistic symbioses adapted to nutrient-poor environments", *Bioscience*, v. 27, n. 7, pp. 454–460, 1977.

[31] FALKOWSKI, P. G., DUBINSKY, Z., MUSCATINE, L., et al. "Light and the bioenergetics of a symbiotic coral", *Bioscience*, v. 34, n. 11, pp. 705–709, 1984.

[32] GLYNN, P. W. "Coral reef bleaching: ecological perspectives", *Coral reefs*, v. 12, pp. 1–17, 1993.

[33] HOEGH-GULDBERG, O. "Climate change, coral bleaching and the future of the world's coral reefs", *Marine and freshwater research*, v. 50, n. 8, pp. 839–866, 1999.

[34] HUGHES, T. P., ANDERSON, K. D., CONNOLLY, S. R., et al. "Spatial and temporal patterns of mass bleaching of corals in the Anthropocene", *Science*, v. 359, n. 6371, pp. 80–83, 2018.

[35] GRAHAM, N. A., WILSON, S. K., JENNINGS, S., et al. "Dynamic fragility of oceanic coral reef ecosystems", *Proceedings of the National Academy of Sciences*, v. 103, n. 22, pp. 8425–8429, 2006.

[36] BAKER, A. C. "Flexibility and specificity in coral-algal symbiosis: diversity, ecology, and biogeography of Symbiodinium", *Annual Review of Ecology, Evolution, and Systematics*, v. 34, n. 1, pp. 661–689, 2003.

[37] MCMANUS, L. C., TEKWA, E. W., SCHINDLER, D. E., et al. "Evolution reverses the effect of network structure on metapopulation persistence", *Ecology*, v. 102, n. 7, pp. e03381, 2021.

[38] MCMANUS, L. C., FORREST, D. L., TEKWA, E. W., et al. "Evolution and connectivity influence the persistence and recovery of coral reefs under climate change in the Caribbean, Southwest Pacific, and Coral Triangle", *Global Change Biology*, v. 27, n. 18, pp. 4307–4321, 2021.

[39] FRANKLIN, E. C., STAT, M., POCHON, X., et al. "GeoSymbio: a hybrid, cloud-based web application of global geospatial bioinformatics and ecoinformatics for Symbiodinium–host symbioses", *Molecular Ecology Resources*, v. 12, n. 2, pp. 369–373, 2012.

[40] WALSWORTH, T. E., SCHINDLER, D. E., COLTON, M. A., et al. "Management for network diversity speeds evolutionary adaptation to climate change", *Nature Climate Change*, v. 9, n. 8, pp. 632–636, 2019.

[41] FULTON, C. J., DEPCZYNSKI, M., HOLMES, T. H., et al. "Sea temperature shapes seasonal fluctuations in seaweed biomass within the Ningaloo coral reef ecosystem", *Limnology and Oceanography*, v. 59, n. 1, pp. 156–166, 2014.